

Wouter van Heijst

The algebraic square peg problem

School of Science

Thesis submitted for examination for the degree of Master of
Science in Technology.

Espoo 18.3.2014

Thesis supervisor and advisor:

Prof. Alexander Engström

Author: Wouter van Heijst

Title: The algebraic square peg problem

Date: 18.3.2014

Language: English

Number of pages: 4+61

Department of Mathematics and Systems Analysis

Professorship: Mathematics

Code: Mat-1

Supervisor and instructor: Prof. Alexander Engström

The square peg problem asks whether every continuous curve in the plane that starts and ends at the same point without self-intersecting contains four distinct corners of some square. Toeplitz conjectured in 1911 that this is indeed the case. Hundred years later we only have partial results for curves with additional smoothness properties.

The contribution of this thesis is an algebraic variant of the square peg problem. By casting the set of squares inscribed on an algebraic plane curve as a variety and applying Bernshtein's Theorem we are able to count the number of such squares. An algebraic plane curve defined by a polynomial of degree m inscribes either an infinite amount of squares, or at most $(m^4 - 5m^2 + 4m)/4$ squares. Computations using computer algebra software lend evidence to the claim that this upper bound is sharp for generic curves.

Earlier work on Toeplitz's conjecture has shown that generically an odd number of squares is inscribed on a smooth enough Jordan curve. Examples of real cubics and quartics suggest that there is a similar parity condition on the number of squares inscribed on some topological types of algebraic plane curves that are not Jordan curves. Thus we are led to conjecture that algebraic plane curves homeomorphic to the real line inscribe an even number of squares.

Keywords: Toeplitz's conjecture, square peg problem, inscribed squares, algebraic plane curves, enumerative algebraic geometry, root counting, Bernshtein's Theorem

Acknowledgements

I thank my advisor Alexander Engström for suggesting the algebraic square peg problem as a thesis topic, and for his continued guidance. The past and present members of the research group are due thanks for discussions and insight about polytopes, curves, squares and other mathematical objects. The feedback from my proofreaders has been uniformly helpful, thank you.

Finally I thank my wife Anu for patiently enduring my preoccupation with mathematics during the conception and writing of this thesis.

Otaniemi, 18.3.2014

Wouter van Heijst

Contents

Abstract	ii
Acknowledgements	iii
1 Introduction	1
2 Background	2
2.1 Algebra	3
2.2 Polytopes	6
2.3 Varieties	14
3 Problem formulation	19
4 An upper bound on the number of isolated squares	21
4.1 The effect of naive generators	23
4.2 A better choice of generators	24
4.3 Monomials present in g_i	24
4.3.1 Example for a fourth degree curve	26
4.4 Newton polytope shapes	27
4.5 Minkowski sum shapes	31
4.6 Minkowski sum volumes	33
4.7 Applied BKK bound	35
5 Experimental evidence for the number of complex squares	36
6 Illustrative examples of real squares	36
6.1 Topological types of curves with a possible parity condition on the number of inscribed squares	39
6.1.1 One topological line inscribing an even number of squares . . .	39
6.1.2 Pairs of ovals inscribing an even number of squares	40
6.1.3 An oval and two lines inscribing an odd number of squares . .	40
6.2 Topological types of curves lacking a parity condition on the number of inscribed squares	44
6.2.1 Squares inscribed on one oval and one line	44
6.2.2 Squares inscribed on two lines	45
6.2.3 Squares inscribed on three lines	47
6.2.4 Squares inscribed on an oval and three lines	48
7 Concluding remarks	50
References	50
Appendix	52
Table of polynomials	52
Code	55

1 Introduction

Toeplitz conjectured in 1911 that every continuous closed curve in the plane that does not self-intersect, also known as a Jordan curve, contains all four corners of some square. More than a hundred years have passed since the statement of Toeplitz's conjecture; various partial results assuming the curve satisfies additional smoothness properties have been proven, but in full generality the problem remains unsolved.

Why look at squares? The conjecture does not hold if squares are replaced with regular polygons with more than four vertices; Eggleston [5] gave an example of a convex curve, a curve that is the boundary of a convex region of the plane, that does not inscribe any regular polygon with more than four vertices. On the other hand, the conjecture does hold if squares are replaced by triangles or rectangles; Nielsen [16] showed that any Jordan curve inscribes a triangle and Vaughan, by way of Meyerson [15], proved that every Jordan curve inscribes some rectangle. Vaughan's proof has no control over the aspect ratio of the inscribed rectangle. Both these cases are discussed in Igor Pak's online book "Lectures on Discrete and Polyhedral Geometry" [17, Section 5, "Inscribed and circumscribed polygons"]. We shall concern ourselves in this thesis with the special case of inscribing a rectangle with prescribed equal aspect ratio, otherwise known as a square. See Matschke's survey paper [14, Section 4] for further problems related to the square peg problem.

Initial publications on the square peg problem, as Toeplitz's conjecture has become known, were made by Emch; who proved the existence of an inscribed square on convex curves [7] in 1913 and three years later for piecewise analytic curves with a finite number of singularities [8]. According to Matschke [14, Emch's proof], implicit in Emch's work is the understanding that a generic curve inscribes an odd number of squares. Since zero is not an odd number, such a parity argument implies the existence of at least one inscribed square, thereby proving Toeplitz's conjecture for these restricted classes of curves. The sense of genericity is important; Popvasilev showed that for any natural number n , there exists a continuous curve that inscribes exactly n squares [19].

Further work on the square peg problem came from, among others, the hands of Jerrard [13], and Stromquist [26]. Jerrard's proof for analytic curves and Stromquist's proof for locally monotone curves both show that generically the number of squares inscribed on a smooth enough curve is odd. Stromquist's locally monotone curves is one of the largest classes for which Toeplitz's conjecture is known to hold. In more recent years Pak [18] has given an elementary proof for piecewise linear curves while Matschke [14, Theorem 3.3] has generalized the square peg problem to arbitrary metric spaces.

We refer readers interested in the history of the square peg problem to Matschke's survey paper [14] or the papers of Sagols and Marín [22, Section 1] and Pak [18, Section 3].

In this thesis we shall employ algebra, rather than the analytical and topological methods of the above approaches, to count the number of squares that may be inscribed on a curve. Thus the class of curves we consider is that of the alge-

braic plane curves, which are curves defined by the vanishing of a polynomial in two variables. These are no longer necessarily Jordan curves, but exhibit interesting behaviour nonetheless. The main result of this thesis, Theorem 4.8, states that an algebraic plane curve of degree m inscribes at most $(m^4 - 5m^2 + 4m)/4$ isolated squares. Section 5 on page 36 provides some evidence for the claim that a generic complex algebraic plane curve inscribes exactly $(m^4 - 5m^2 + 4m)/4$ squares. The behaviour of real algebraic plane curves is less clear, examples of real algebraic plane curves of different topological types inscribing various numbers of squares are listed in Section 6 on page 36. Those examples form the basis for three conjectures in Section 7 on page 50, similar to the results from Emch, Jerrard, and Stromquist that a generic Jordan curve inscribes an odd number of squares. The most striking of these, to the author's eyes at least, is the conjecture that an algebraic plane curve homeomorphic to the real line inscribes an even number of squares.

The outline of this thesis is as follows: In Section 2 we recall some algebra, polytope theory, and algebraic geometry to support understanding of the statement of Bernshtein's Theorem, Theorem 4.1. In Section 3 on page 19 we formulate the algebraic square peg problem; we parametrize a complex square in Definition 2 as a 4-tuple (a, b, c, d) where (a, b) is the center of the square and the four corners are offset from the center by (c, d) , $(-d, c)$, $(-c, -d)$ and $(d, -c)$. Evaluating a polynomial f at these four corners gives the four generators of the corner ideal that describes all squares inscribed on the algebraic plane curve defined by f . Bernshtein's Theorem provides an estimate on the number of isolated solutions to this system of four polynomials. While the immediate estimate is no better than Bézout's bound, in Section 4 on page 21 we show that a different choice of generators yields Newton polytopes whose mixed volume gives exactly the bound $(m^4 - 5m^2 + 4m)/4$ on the number of inscribed isolated squares. That this bound is tight, at least for low degrees, is exhibited by experimental data in section 5 on page 36. In Section 6 on page 36 we picture simple real algebraic plane curves of degrees three to eight inscribing varying numbers of squares. Finally we discuss some directions for future work in Section 7 on page 50.

2 Background

The square peg problem is inherently a geometric problem: Whether a curve inscribes a square depends on the lengths of and angles between line segments connecting pairs of points on the curve. Considering squares inscribed on algebraic curves allows us to view the square peg problem as an algebraic problem as well. The gain of this approach is that we can use algebraic tools, such as Bernshtein's Theorem, to make definite statements about the set of inscribed squares.

The main result of this thesis, Theorem 4.8, states that the number of isolated squares inscribed on an algebraic curve of degree m is at most $(m^4 - 5m^2 + 4m)/4$. The proof of this result depends on Bernshtein's Theorem, Theorem 4.1, which bounds the number of solutions to a polynomial system of equations by the mixed

volume of the Newton polytopes of the generators of that polynomial system. The purpose of this background section is to present enough knowledge about these concepts such that readers who were not previously familiar with them can understand the statement of Bernshtein's Theorem.

In Section 2.1 we will recall some basic facts about polynomials and ideals of polynomial rings. The fact that each ideal is finitely generated is known as Hilbert's Basis Theorem (Lemma 2.1).

We discuss convexity, polytopes, simplices, Minkowski sums, Schlegel diagrams, normal fans, Newton polytopes and the definition of the mixed volume in Section 2.2 on page 6.

In Section 2.3 on page 14 we mention the Nullstellensatz, which states that over an algebraically closed field, the radical of any ideal defining a variety is exactly the ideal of polynomials vanishing on that variety. We also show that varieties consist of a finite number of irreducible components (Lemma 2.7), and the fact that the saturation of an ideal I with respect to an ideal J corresponds to the difference in varieties of I and J (Lemma 2.8). These two results will be used in Section 4 on page 21 and Section 5 on page 36 to ensure that we are counting all the non-degenerate squares inscribed on an algebraic plane curve.

The algebra and results on varieties follow the expositions of Cox [4] and Eisenbud [6]. The polytope theory derives from Ziegler's book on polytopes [27, Chapters 0, 1, 2, 5 and 7]. Definition 1 of the mixed volume is taken from Schneider's book on convex bodies [23].

Readers familiar with these topics can safely skip this background section and proceed immediately to Section 3 on page 19.

2.1 Algebra

Algebraic plane curves are a special case of geometric objects called varieties. Varieties are defined by the vanishing of a set of polynomials; in the case of plane curves these are polynomials in two variables. Before we discuss these algebraic geometric objects in Section 2.3 on page 14, we define some basic notions concerning polynomials and their natural environments, polynomial rings.

Let x_1, \dots, x_n be n independent variables and $\alpha \in \mathbb{N}^n$ a tuple of nonnegative integers. A *monomial* $x^\alpha = x_1^{\alpha_1} \dots x_n^{\alpha_n}$ is a product of powers of the variables x_i . The degree of a monomial x^α is the sum $\alpha_1 + \dots + \alpha_n$ of the entries of its exponent. A *polynomial* over a field \mathbb{k} in x_1, \dots, x_n is a finite sum $\sum_{\alpha \in \mathbb{N}^n} c_\alpha x^\alpha$ of monomials where the coefficients c_α are elements of the field \mathbb{k} . The *total degree* (or simply degree) $\deg f$ of a polynomial is the maximal degree of its monomials; the degree of $3xy^2 - xy$ is three due to the exponent $(1, 2)$ of the monomial xy^2 .

The collection of all polynomials in x_1, \dots, x_n over \mathbb{k} , denoted $\mathbb{k}[x_1, \dots, x_n]$, is called a *polynomial ring*. This terminology is justified, as multiplication and addition of polynomials equip $\mathbb{k}[x_1, \dots, x_n]$ with the structure of a ring. A *monomial ordering* $<$ on a polynomial ring is a binary relation with the following properties for any distinct exponents $\alpha, \beta \in \mathbb{N}^n$,

1. either $x^\alpha < x^\beta$ or $x^\beta < x^\alpha$ (linear ordering)
2. $x^\alpha < x^\beta$ implies $x^{\alpha+\gamma} < x^{\beta+\gamma}$ for any $\gamma \in \mathbb{N}^n$.
3. $1 < x^\gamma$ for any nonzero $\gamma \in \mathbb{N}^n$ (well-ordering).

As usual with orderings we write $x^\alpha \leq x^\beta$ if either $x^\alpha = x^\beta$ or $x^\alpha < x^\beta$. The leading monomial $\mathbf{LM}_<(f)$ of a polynomial f compares greater than any other monomial of f with respect to the ordering $<$. The coefficient of the leading monomial is denoted $\mathbf{LC}_<(f)$. The explicit dependence on the particular ordering $<$ is suppressed if no confusion is likely to arise. There is only one monomial ordering on univariate polynomials, $x^d < x^e$ if $d < e$, but multivariate polynomials admit many different monomial orderings.

Certain subsets of $\mathbb{k}[x_1, \dots, x_n]$ hold special interest for us. A subset $I \subset \mathbb{k}[x_1, \dots, x_n]$ is called an *ideal* if it is closed under multiplication by elements of the polynomial ring and closed under addition by elements of I . These conditions can be compactly stated with set-wise addition and multiplication notation, respectively $\mathbb{k}[x_1, \dots, x_n]I \subset I$ and $I + I \subset I$.

The set $\{0\}$ is an ideal as $0 + 0 = 0$ and $f \cdot 0 = 0$ for any polynomial $f \in \mathbb{k}[x_1, \dots, x_n]$. The set $\{x, y\} \subset \mathbb{k}[x, y, z]$ on the other hand is not an ideal; neither $x + y$ nor xz are contained in $\{x, y\}$, so $\{x, y\}$ violates both closedness properties of an ideal. The set $\{xf \mid f \in \mathbb{k}[x, y]\}$ of “polynomial consequences of x ” is again an ideal of $\mathbb{k}[x, y]$; both the addition of elements $xg + xg' = x(g + g')$ and the multiplication of an element xg with an arbitrary polynomial g' are of the form xf required to be an element of the set.

Any ideal I can be expressed as the consequence of an, a priori possibly infinite, set of generators B_I called a *basis* for I ,

$$I = \langle B_I \rangle = \left\{ \sum_{i=1}^r h_i g_i \mid r \in \mathbb{N}, g_i \in B_I, h_i \in \mathbb{k}[x_1, \dots, x_n] \right\}.$$

The ideals $\{0\}$ and $\{xf \mid f \in \mathbb{k}[x, y]\}$ are generated by single polynomials, 0 and x respectively. Bases are not unique, as the examples $\langle x, y \rangle = \langle x + y, x - y \rangle$ and $\langle x, xy, y \rangle = \langle x, y \rangle$ show. If I has a finite basis I is *finitely generated*.

A ring with the property that every ideal is finitely generated is called *Noetherian*. It is easy to see that all fields are Noetherian; any ideal $I \subset \mathbb{k}$ other than $\langle 0 \rangle$ contains some nonzero element u . Since all nonzero elements of \mathbb{k} are invertible and I is closed under multiplication by field elements, $r = ru^{-1}u \in I$ for all $r \in \mathbb{k}$. But then I is the entire field itself, $I = \langle 1 \rangle$. As all ideals of a field are generated by a single element, any field is clearly Noetherian.

As a consequence of the next lemma, polynomial rings over a field are Noetherian as well.

Lemma 2.1 (Hilbert’s Basis Theorem [6, Theorem 1.2]). *Let R be a Noetherian ring. Then $R[x]$ is Noetherian.*

Proof. Let $I \subset R[x]$ be an ideal. Select elements $f_i \in I$ as follows. If $I = \langle f_1, \dots, f_i \rangle$, stop. Otherwise choose $f_{i+1} \in I \setminus \langle f_1, \dots, f_i \rangle$ of minimal degree.

The leading coefficients of the f_i generate an ideal $\langle \mathbf{LC}(f_1), \mathbf{LC}(f_2), \dots \rangle$ of R . This ideal is finitely generated since R is Noetherian. Let m be the smallest index such that the first m leading coefficients generate the entire ideal of leading coefficients, $\langle \mathbf{LC}(f_1), \dots, \mathbf{LC}(f_m) \rangle = \langle \mathbf{LC}(f_1), \dots \rangle$. We claim that our process must have stopped at f_m , that is, $I = \langle f_1, \dots, f_m \rangle$.

Suppose we had picked an f_{m+1} . By assumption on m the leading coefficient $\mathbf{LC}(f_{m+1})$ can be expressed as a linear combination $\sum_{j=1}^m u_j \mathbf{LC}(f_j)$ of the earlier leading coefficients. The polynomial $g = \sum_{j=1}^m u_j f_j x^{\deg f_{m+1} - \deg f_j}$ has the same degree and leading term as f_{m+1} by construction. Their difference, $f_{m+1} - g$, is of strictly smaller degree than f_{m+1} . By minimality of f_{m+1} , the difference $f_{m+1} - g$ must be an element of $\langle f_1, \dots, f_m \rangle$. As f_{m+1} is the sum of two elements of $\langle f_1, \dots, f_m \rangle$, it must itself be an element of this ideal, which contradicts the choice of f_{m+1} . \square

Hilbert's Basis Theorem is stated for univariate polynomials with coefficients in a Noetherian ring; as we can rewrite a polynomial $\sum c_\gamma x_1^{\gamma_1} \dots x_n^{\gamma_n}$ as a sum $\sum_{i=0}^r (\sum_{\gamma_n=i} c_\gamma x_1^{\gamma_1} \dots x_{n-1}^{\gamma_{n-1}}) x_n^i$ of monomials in x_n with coefficients in $\mathbb{k}[x_1, \dots, x_{n-1}]$, the polynomial ring $\mathbb{k}[x_1, \dots, x_n] = \mathbb{k}[x_1, \dots, x_{n-1}][x_n]$ is Noetherian as well.

A sequence (A_1, A_2, \dots) of nested sets is called *ascending* if $A_i \subset A_{i+1}$ and *descending* if $A_i \supset A_{i+1}$. Such a sequence terminates, or stabilizes, if the tail of the sequence is constant, that is, $A_n = A_N$ for some $N \in \mathbb{N}$ and all $n \geq N$. If every ascending chain of ideals of a ring R terminates, R is said to satisfy the *Ascending Chain Condition* (ACC). The Ascending Chain Condition on a ring and a ring being Noetherian are two different ways of looking at the same property.

Lemma 2.2. *The Ascending Chain Condition and being Noetherian are equivalent.*

Proof. Let R be a Noetherian ring and let $I_1 \subset I_2 \subset \dots$ be an ascending chain of ideals. The union $I = \cup_1^\infty I_i$ is again an ideal, since $f, g \in I$ implies that $f, g \in I_r$ for some r large enough. By assumption I is finitely generated, say $I = \langle f_1, \dots, f_m \rangle$. The chain terminates at the smallest index j such that $f_1, \dots, f_m \in I_j$.

Assume that a ring R has the Ascending Chain Condition and let I be an ideal of R . Pick $f_1 \in I$ and $f_{i+1} \in I \setminus \langle f_1, \dots, f_i \rangle$. The ideals $I_i = \langle f_1, \dots, f_i \rangle$ so constructed form an ascending chain. By the ACC the chain terminates, providing a finite set of generators for I . \square

In the sequel we separate non-degenerate squares from degenerate squares inscribed on a curve by taking the difference of varieties. The corresponding algebraic operation is called saturation, which is phrased in terms of colon ideals. Let $I, J \subset \mathbb{k}[x_1, \dots, x_n] = R$ be ideals. The *colon ideal* $I : J$ is the set $\{f \in R : fJ \subset I\}$. The colon ideal $\langle xy \rangle : \langle y \rangle$ contains all polynomials f such that $fy \in \langle xy \rangle$. It does not contain the polynomial 1, as y is not an element of $\langle xy \rangle$. It does contain x , and it is not hard to show that $\langle xy \rangle : \langle y \rangle = \langle x \rangle$.

Recall that the notation J^m denotes the set of all products $\prod_{i=1}^m j_i$ with m factors from J . The *saturation* $I : J^\infty$ of I with respect to J is the ideal $\bigcup_{m=0}^\infty I : J^m$. The colon ideals $I : J^m$ form an ascending chain; as I is an ideal and thus closed under multiplication by the ring, the condition $fJ \subset I$ implies that $fJ^2 \subset I$. The ascending chain $I \subset I : J \subset I : J^2 \subset \dots$ terminates because polynomial rings are Noetherian, and thus the saturation $I : J^\infty = I : J^M$ for some $M \in \mathbb{N}$.

For multivariate polynomials it is often convenient to think about all the monomials of a certain degree separately. The monomials of a fixed degree form a basis for the vector space of all homogenous polynomials of that degree. A general approach for grouping objects with the same properties together is to work with a grading. A *grading* of a ring R is a decomposition of R as a direct sum $R_0 \oplus R_1 \oplus \dots$ into abelian groups R_i with the property that $R_i R_j \subset R_{i+j}$. An element $f \in R_k$ is called a *homogeneous* element, or a *form*, of degree k . A polynomial ring has a grading by total degree where the homogeneous polynomials of degree k are sums of monomials of total degree k . The homogeneous parts of a polynomial f are homogeneous elements $f_i \in R_i$ such that $f_1 + \dots + f_{\deg f} = f$. The three homogeneous parts of $f = 3x^3y^3 + xy + 2x^2 + 1$ are the forms $3x^3y^3$, $xy + 2x^2$ and 1.

2.2 Polytopes

Bernshtein's Theorem is stated in terms of polynomials, varieties, Newton polytopes and mixed volumes. We discussed polynomials in the previous section and will discuss varieties in the next section. The current section contains the definition of mixed volume and enough polytope theory to understand the statement of Bernshtein's Theorem, as well as the proofs in Section 4 on page 21.

Throughout this section V denotes the ambient vector space containing the geometric objects of interest. Its dual space V^* consists of all linear functionals $\alpha: V \rightarrow \mathbb{k}$. The notation $\langle \alpha, v \rangle$ denotes the functional pairing $\langle \alpha, v \rangle = \alpha(v)$ as well as the inner product on V by identifying the functional $\alpha \in V^*$ with a suitable vector $\alpha \in V$. As V will always be finite-dimensional in this thesis, no confusion is likely to arise. The standard basis vectors e_i of V are unit vectors whose i -th coordinate is one. The standard basis vectors of the plane are $e_1 = (1, 0)$ and $e_2 = (0, 1)$.

Polytopes are a particular nice class of convex geometric objects. A set S is *convex* if it contains all line segments between its constituent points. Equivalently, convexity of S can be expressed as the property that S contains all the convex combinations of its elements. A finite sum $\sum_{i=1}^r t_i s_i$ is a *convex combination* of elements s_i of S if all the t_i are non-negative and sum to one. This leads us to the definition of the *convex hull* of S , the set of all convex combinations of elements of S ,

$$\text{conv} S = \left\{ \sum_{i=1}^r t_i s_i \mid r \in \mathbb{N}, s_i \in S, t_i \geq 0, \sum_{i=1}^r t_i = 1 \right\}.$$

If we do not require that the t_i are non-negative, a finite sum $\sum_{i=1}^r t_i s_i$ such that the t_i sum to one is an *affine combination* of the elements s_i . The *affine hull*

is defined analogously to the convex hull. The affine hull of a subset S of V is the smallest *affine* subspace of V that contains S . If the affine subspace contains the element 0 it is also a linear subspace of V . If 0 is not contained in an affine subspace A , then A is the translation of some linear subspace of V . The dimension of an affine subspace is the dimension of the linear subspace it is a translate of. Consider affine space a linear space where we have forgotten how to distinguish the zero element.

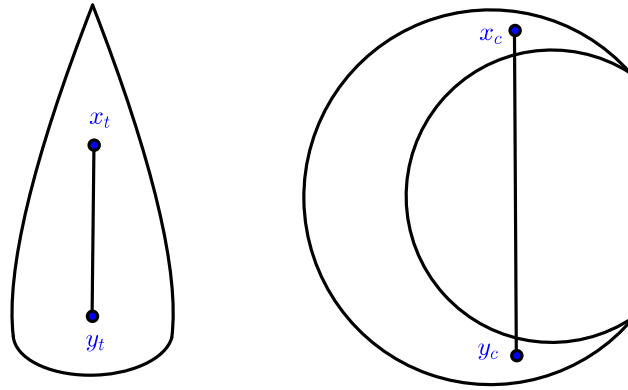


Figure 1: The teardrop is convex because it contains every line segment between two of its points. The crescent is not convex.

The line $y = x + 1$ is not a linear subspace of \mathbb{R}^2 since it does not contain the origin, but it is an affine subspace. For linear subspaces we are used to the concept of linear independence, affine subspaces have a similar concept of affine independence. A set $\{p_1, \dots, p_r\} \subset V$ of points is *affinely independent* if no p_i is contained in affine hull spanned by the other p_j . Linear independence implies affine independence, but not vice versa. The set $\{(1, 0), (0, 1), (1, 1)\}$ is affinely independent since a line through two of the points does not contain the third. The set $\{(1, 0), (0, 1), (1/2, 1/2)\}$ is affinely dependent as the three points are collinear. These affine hulls are depicted in Figure 2.

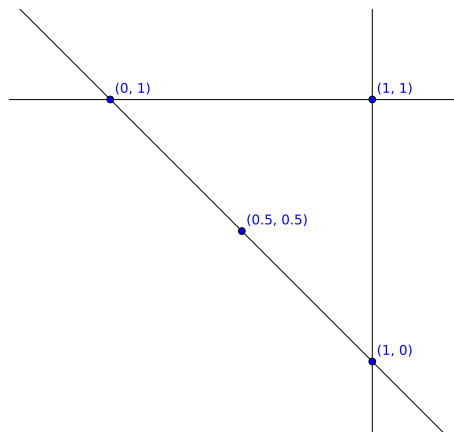


Figure 2: The affine hull of a pairs of points, or collinear points, is a line.

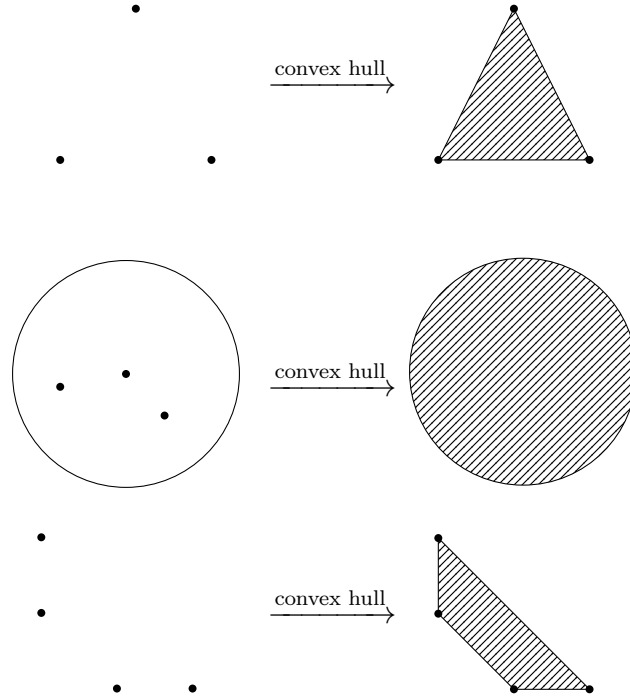


Figure 3: Subsets of the plane and their convex hulls. The disc is not a polytope, the other two convex hulls are polytopes.

Points, edges, triangles, tetrahedra and their higher-dimensional generalizations have the property that their vertices are affinely independent; an n -simplex is the convex hull of $n + 1$ affinely independent points. The convex hull of the origin and the n standard basis vectors e_i of an n -dimensional vector space is an n -simplex. In one, two and three dimensions the volumes of such simplices are 1, $1/2$ and $1/6$. Volume is invariant under translation, so the volume of an n -simplex with vertices v_0, v_1, \dots, v_n is the same as that of the n -simplex with vertices $0, v_1 - v_0, \dots, v_n - v_0$. The matrix with column vectors $v_i - v_0$ maps the vertices of $\text{conv}(0, e_1, \dots, e_n)$ to the vertices $\text{conv}(0, v_1 - v_0, \dots, v_n - v_0)$. The volume of the second simplex is proportional to the volume of the first simplex, as the determinant of a matrix can be interpreted as a scaling factor in volume. According to Stein [25], the volume of a general n -simplex with vertices v_0, v_1, \dots, v_n is

$$\frac{1}{n!} \left| \det \begin{pmatrix} v_1 - v_0 & v_2 - v_0 & \dots & v_n - v_0 \end{pmatrix} \right|.$$

A *polytope* is the convex hull of a *finite* set of points, not necessarily affinely independent. Figure 3 depicts some examples and non-examples of polytopes.

The *Minkowski (or vector) sum* of two sets S and T is the set $S + T = \{s + t : s \in S, t \in T\}$ of sums of their elements. The Minkowski sum is a well-defined binary operation on the space of convex objects as well as the space of polytopes. Let S and T be two convex sets. The cartesian product $S \times T$ is again convex and the map

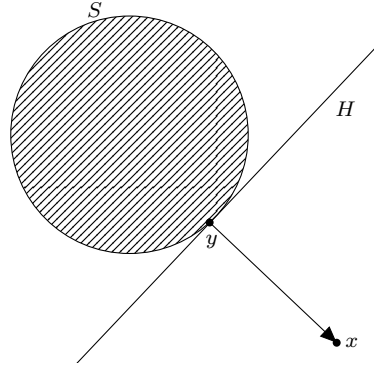


Figure 4: The supporting hyperplane H separates the closed convex set S from any point x outside of S .

$(s, t) \mapsto s + t$ is linear so in particular it preserves convex combinations. Assume furthermore that S and T are the convex hulls of finite sets of points $\{s_1, \dots, s_p\}$ and $\{t_1, \dots, t_q\}$. An arbitrary point $s + t = \sum_1^p \lambda_i s_i + \sum_1^q \mu_j s_j$ is the convex combination $\sum_{i,j} \lambda_i \mu_j (s_i + t_j)$ so $S + T$ is the convex hull of the finite set $\{s_1, \dots, s_p\} + \{t_1, \dots, t_q\}$ and hence a polytope.

A different viewpoint defines a polytope as the bounded intersection of a finite number of halfspaces. The equivalence between these two viewpoints is a fundamental result in polytope theory, see Ziegler [27, Theorem 1.1]. Obtaining a vertex description from a halfspaces description and vice-versa is a hard problem in general. For the specific polytopes occurring in this thesis both descriptions are at hand.

A hyperplane $H_{\alpha,c} = \{x \in V : \langle \alpha, x \rangle = c\} \subset V$ is an affine subspace of codimension one with normal vector α . The closed halfspaces $H_{\alpha,c}^- = \{x \in V : \langle \alpha, x \rangle \leq c\}$ and $H_{\alpha,c}^+ = \{x \in V : \langle \alpha, x \rangle \geq c\}$ contain all the points to one side of $H_{\alpha,c}$ in addition to the hyperplane itself.

A hyperplane H *supports* a convex set S at the point v if H touches S at the point v and S lies on one side of H , that is, $v \in H \cap S$ and either $S \subset H^-$ or $S \subset H^+$. It is allowed for S to lie within H , the line segment $\{(x, y) \mid x \geq 0, y \geq 0, x + y = 1\}$ is supported by the hyperplane $x + y = 1$ at any of its points.

If $H_{\alpha,c}$ supports S and $S \subset H_{\alpha,c}^-$ then $H_{\alpha,c}^-$ is a supporting halfspace of S with outward normal vector α . If the convex set S is also closed, then for any x outside of S there is a unique point $y \in S$ that is closest to x . The hyperplane through y that is perpendicular to the line segment between x and y supports S at y . This construction, depicted in Figure 4, shows that for each point x outside of S there is a halfspace H^- that contains S but not x , and thus every nonempty closed convex set is the intersection of its supporting halfspaces [23, Corollary 1.3.5]. Let $P = H_1^- \cap \dots \cap H_r^-$ be a polytope defined as the intersection of r halfspaces, where r is minimal. An intersection of P with multiple halfplanes H_i yields a subset of P called a *face*. A face of dimension i is called an i -face. Every polytope trivially has itself as a face. Faces that are strict subsets of the polytope are *proper* faces. Special terminology is used for 0-faces (*vertices*), 1-faces (*edges*) and the proper faces of largest dimension (*facets*). An n -dimensional polytope is *simple* if all its vertices

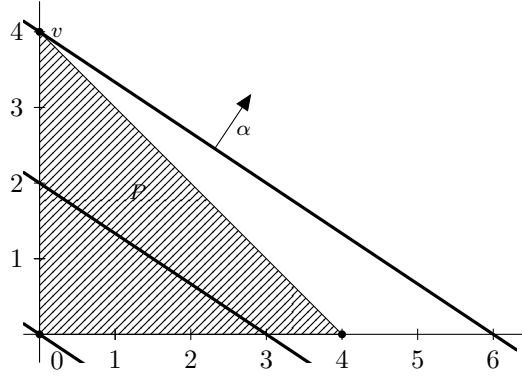


Figure 5: The face v of the triangle P is the maximizer $F_P(\alpha)$ of P with respect to α .

are contained in the minimum of n facets. A three-dimensional cube is simple, since each vertex is contained in three facets, but a pyramid with a square base is not simple as the apex is contained in four facets.

There is a dual way of thinking of the faces of a polytope, for a functional $\alpha \in V^*$ let $M_P(\alpha) = \max_{v \in P} \langle \alpha, v \rangle$ denote the maximum value that α attains on P . The maximizer $F_P(\alpha)$ of P with respect to α is the subset of P where α attains the maximal value $M_P(\alpha)$,

$$F_P(\alpha) = \left\{ v \in P \mid \langle \alpha, v \rangle = \max_{w \in P} \langle \alpha, w \rangle \right\}.$$

One way to envision the maximizer of P with respect to α is to picture sliding the halfplane perpendicular to α along its normal in the positive direction, see Figure 5. As the hyperplane progresses along α there is a critical point where the intersection with P becomes empty. The last non-empty intersection is the set $F_P(\alpha)$.

Lemma 2.3. *The faces of a full-dimensional polytope P are exactly the sets of maximizers $\{v \in P \mid \langle v, \alpha \rangle = \max_{w \in P} \langle w, \alpha \rangle\}$ where α ranges over all functionals on the ambient vector space containing the polytope.*

Proof. Let H_1, \dots, H_r be a set of facet-defining hyperplanes of P with outward normals n_1, \dots, n_r . The polytope itself maximizes the zero functional. Facets are the maximizers with respect to their facet normals. Any lower dimensional faces are intersections of multiple facets.

Assume that the intersection $H_1 \cap \dots \cap H_n$ is a face F of P . Then for $\alpha \in \text{cone}\{n_1, \dots, n_r\} = \{\sum t_i n_i \mid t_i \geq 0\}$ the face F is a subset of the maximizer $F_P(\alpha)$. If one of the t_i is zero, the containment is strict, but if all t_i are positive then any point x outside of any of the H_i is not an element of the maximizer $F_P(\alpha)$. Hence the face F is equal to $F_P(\alpha)$. \square

The *normal cone* of a face F is the set of functionals $\{\alpha \in V^* \mid F_P(\alpha) = F\}$ that attain their maximal value precisely on F . Identifying the functionals $\alpha \in V^*$ with

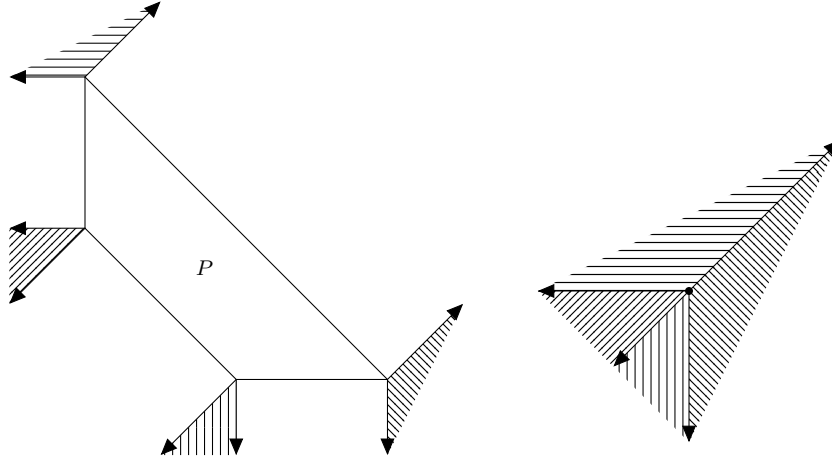


Figure 6: The normal fan of P partitions the plane into normal cones of all the faces of P .

vectors $\alpha \in V$ such that $\alpha(v) = \langle \alpha, v \rangle$ for every $v \in V$, these normal cones can be thought of as geometric objects living in the same space as F .

The *normal fan* of the polytope P is the collection of the normal cones of all faces of P ; it partitions V^* into cones, see Figure 6. Scaling a polytope by a positive scalar does not change the normal fans, as is clear from the equality $\lambda P = \{\lambda x : Ax \leq b\} = \{x : Ax \leq \lambda b\}$.

Let P be an n -dimensional polytope. A *triangulation* S of P is a decomposition of P into simplices of dimension n with mutually disjoint interiors, Figure 7 on the next page shows triangulations for a square and a triangular prism.

Lemma 2.4. *Let v be a vertex of a polytope P and for F a facet of P not containing v let S_F be a triangulation of F . Then the union*

$$\bigcup_F \{\text{conv}(v, S) \mid S \in S_F\}$$

of the convex hulls of v with each simplex in a triangulation of a face of F not containing v , is a triangulation of P .

Proof. Let $x \in P$ be distinct from v . The ray from v to x exits P in some face F not containing v and thus intersects some simplex $\sigma \in S_F$. The convex hull $\text{conv}(v, \sigma)$ of v and σ contains x by convexity. As v is affinely independent from σ , the simplex $\text{conv}(v, \sigma)$ is full-dimensional.

Suppose the ray through x intersects two distinct simplices σ and τ . Then x is contained in $\text{conv}(v, \sigma \cap \tau)$. Since σ and τ share no interior points, the dimension of the intersection $\sigma \cap \tau$ is at most $n - 2$. The dimension of $\text{conv}(v, \sigma \cap \tau)$ is then at most $n - 1$, so $\text{conv}(v, \sigma)$ and $\text{conv}(v, \tau)$ have disjoint interiors. \square

Lemma 2.4 suggests an algorithm for triangulating a polytope. Starting out with a pair (P, v) , recursively triangulate the facets of P not containing v to obtain the

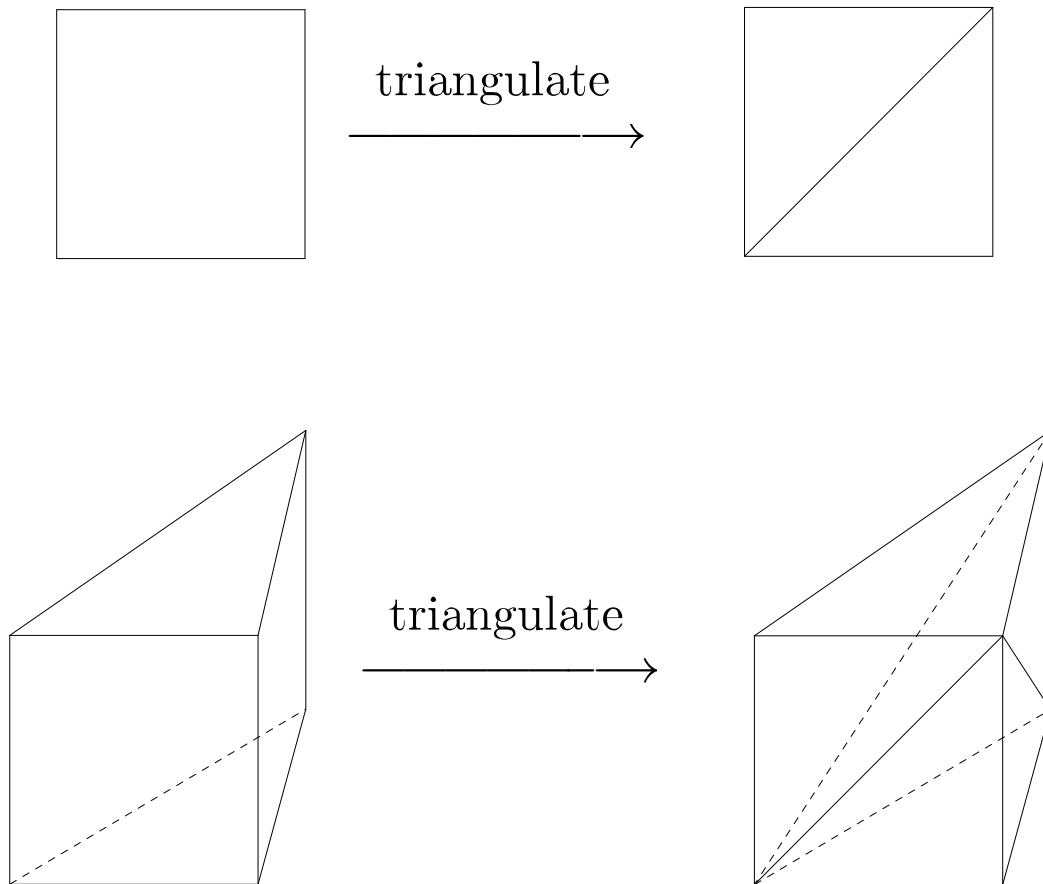


Figure 7: Triangulations of a square and a triangular prism.

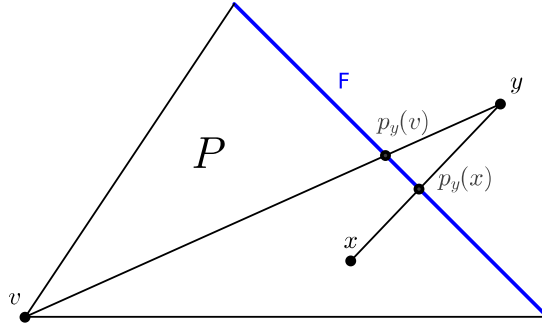


Figure 8: A Schlegel diagram of a polytope P is obtained by projecting P onto a facet F using the projection p_y .

triangulations S_F . This algorithm is known as the Cohen & Hickey algorithm [2, Section 3.1] and will be used in Corollary 4.7 to calculate the volume of a Minkowski sum.

So far we have pictured polytopes of dimension zero, one, two and three. The polytopes playing a main role in this thesis are four-dimensional. One way to visualize four-dimensional polytopes is by using Schlegel diagrams. The idea is to project a polytope onto one of its facets, see Figure 8.

Let y lie beyond a facet F of a polytope P . The projection $p_y(x)$ of $x \in P$ onto F is the intersection of the line segment between x and y with F . The *Schlegel diagram* $\mathcal{D}(P, F)$ of P based at the facet F is the image of all the proper faces of P , other than F , under the projection map p . Its usefulness comes from the fact [27, Proposition 5.6] that although $\mathcal{D}(P, F)$ is of smaller dimension than the original polytope, the combinatorial structures of P and the Schlegel diagram are equivalent. This allows one to read off the face structure of a four-dimensional polytope from a three-dimensional picture. The Schlegel diagrams in this thesis are Figure 16 on page 29 and Figure 17 on page 29.

The concept of mixed volume was introduced by Minkowski in the early 1900s. For our purposes the mixed volume serves only as a computational tool. In the literature various definitions of the mixed volume abound. The following definition as used by Schneider [23], Bernshtein [1] and Huber and Sturmfels [12] is convenient for root counting.

Definition 1 (Mixed volume [23, Theorem 5.1.6]). *Let $P_1, \dots, P_n \subset \mathbb{R}^n$ be n polytopes. Their mixed volume $MV(P_1, \dots, P_n)$ is the coefficient of the monomial $\lambda_1 \dots \lambda_n$ appearing in the expression for the n -dimensional Euclidean volume $\text{Vol}_n(\lambda_1 P_1 + \dots + \lambda_n P_n)$ of the Minkowski sum of the P_i scaled by factors λ_i .*

The process of calculating the mixed volume of two rectangles is depicted in Figure 9 on the next page.

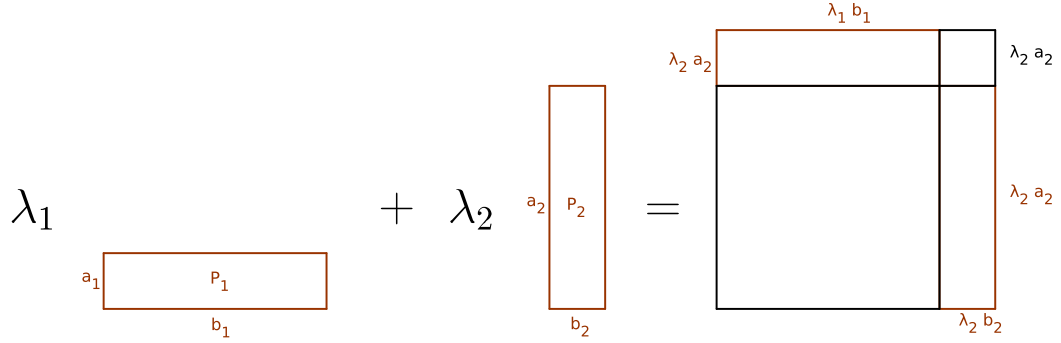


Figure 9: The mixed volume $MV(P_1, P_2)$ of the polytopes P_1 and P_2 is the coefficient of $\lambda_1\lambda_2$ in the expression $\lambda_1^2\text{Vol}(P_1) + \lambda_2^2\text{Vol}(P_2) + \lambda_1\lambda_2(a_1b_2 + a_2b_1)$ for the volume of the Minkowski sum $P_1 + P_2$.

Before we move on to varieties, the last polytopal concept occurring in the statement of Bernstein's Theorem is the concept of a Newton polytope. Let $f = \sum_{\gamma} c_{\gamma} x^{\gamma} \in \mathbb{k}[x_1, \dots, x_n]$ be a polynomial. The *Newton polytope* $\mathcal{N}(f)$ of f is the convex hull of the exponents of the monomials of f , $\mathcal{N}(f) = \text{conv}\{\gamma \in \mathbb{N}^n \mid c_{\gamma} \neq 0\}$.

Example 2.5. The Newton polytopes of $\lambda_{00} + \lambda_{10}x + \lambda_{12}xy^2$ and $\mu_{10}x + \mu_{30}x^3 + \mu_{01}y + \mu_{03}y^3 + \mu_{11}xy$ are depicted in Figure 10. The points (i, j) in the Newton polytopes that are an exponent of a monomial $x^i y^j$ are labeled with the corresponding term.

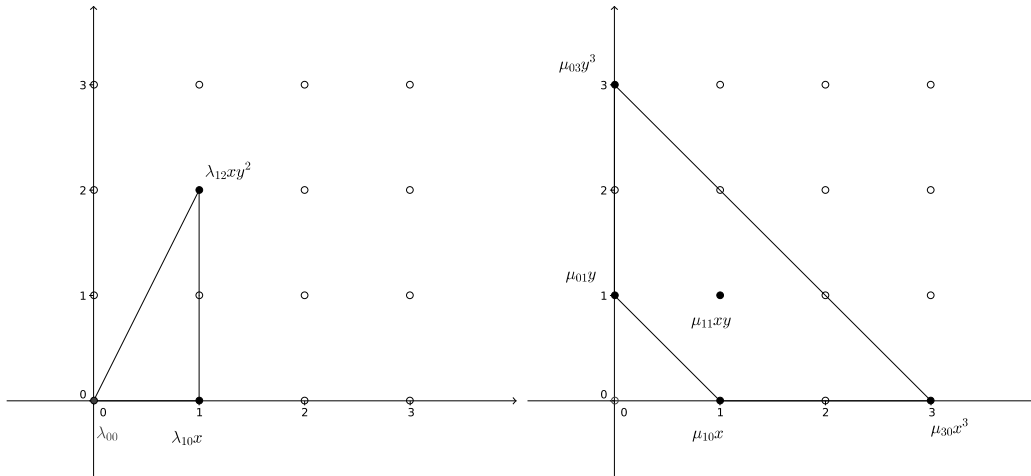


Figure 10: Newton polytopes of the polynomials $\lambda_{00} + \lambda_{10}x + \lambda_{12}xy^2$ and $\mu_{10}x + \mu_{30}x^3 + \mu_{01}y + \mu_{03}y^3 + \mu_{11}xy$.

2.3 Varieties

An algebraic curve and the set of squares inscribed on such a curve are both examples of varieties. Varieties are geometric objects we can describe well by ideals of polynomials vanishing on the variety. This connection enables the use of algebraic tools from the Algebra background section to answer questions of geometry. The

Ascending Chain Condition allows us to show that varieties consist of a finite number of irreducible components; the difference of varieties defined by ideals I and J corresponds to the variety defined by the saturation $I : J^\infty$.

Algebraic geometry is pursued over any field, be it finite or infinite, a subfield of \mathbb{C} or something more exotic. The concrete fields used in the applications in this thesis are the rationals \mathbb{Q} , the reals \mathbb{R} and the complex numbers \mathbb{C} . All of them are infinite fields, which makes some reasoning easier. The complex numbers additionally have the property that they are *algebraically closed*, any nonconstant polynomial with complex coefficients has a complex root. Many proofs that work for the complex numbers, such as the Strong Nullstellensatz, only depend on the fact that the field of complex numbers is algebraically closed. We shall state such results for an arbitrary algebraically closed field.

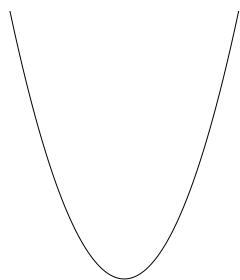
Let $f_1, \dots, f_r \in \mathbb{k}[x_1, \dots, x_n]$ be a set of polynomials. The set of points $(x_1, \dots, x_n) \in \mathbb{k}^n$ simultaneously satisfying the system of equations

$$f_1(x_1, \dots, x_n) = 0, \dots, f_r(x_1, \dots, x_n) = 0,$$

is called the *variety* defined by $\{f_1, \dots, f_r\}$, denoted $\mathbf{V}(f_1, \dots, f_r)$. Linear and affine subspaces are familiar examples, both defined by collections of linear polynomials. Conics, finite sets of points, and graphs $y = f(x_1, \dots, x_n)$ of polynomials are other examples the reader may have seen before. Some varieties and non-varieties are depicted in Figure 11 on the next page. An algebraic plane curve is a variety defined by the vanishing of a single polynomial in two variables. The line through the origin with slope one is an algebraic curve defined by the vanishing of the polynomial $x - y$. The unit circle is defined by the vanishing of the polynomial $x^2 + y^2 - 1$.

The smallest variety V that contains a set S is called the *Zariski closure* \bar{S} of S . The Zariski closure of a point is just the point, as it is already a variety. The Zariski closure of the integers is all of \mathbb{R} , as any polynomial that vanishes on all integers will vanish on all real numbers.

The polynomials f_1, \dots, f_r have the property that they vanish on the variety $\mathbf{V}(f_1, \dots, f_r)$ by construction. The collection $\mathbf{I}(V)$ of all polynomials vanishing on a variety V is called the *ideal of V* . One checks that $\mathbf{I}(V)$ indeed has the structure of an ideal as defined in Section 2.1 on page 3. Any $\mathbb{k}[x_1, \dots, x_n]$ -linear combination of f_1, \dots, f_r vanishes on $\mathbf{V}(f_1, \dots, f_r)$ so we see that $\langle f_1, \dots, f_r \rangle \subset \mathbf{I}(\mathbf{V}(f_1, \dots, f_r))$. That the containment can be strict is illustrated by the ideal $\langle x^2 \rangle \subset \mathbb{k}[x]$; the only point where x^2 is zero is the origin, so $\mathbf{V}(x^2) = \{0\}$. The two monomials of $\mathbb{k}[x]$ not contained in $\langle x^2 \rangle$ are x and 1 . The constant monomial 1 does not vanish anywhere, but x also vanishes at the origin, so $\mathbf{I}(\{0\}) = \langle x \rangle$. There is another relation between the previous two ideals: $\langle x \rangle$ is the radical of $\langle x^2 \rangle$. The *radical* \sqrt{I} of an ideal I is the ideal $\{f \mid f^m \in I, m \in \mathbb{N}\}$ of all polynomials that occur in I to some non-negative power. It is always true that $\sqrt{I} \subset \mathbf{I}(\mathbf{V}(I))$, but when \mathbb{k} is not algebraically closed equality is not guaranteed. If \mathbb{k} is algebraically closed, it is true that the radical of an ideal I contains all polynomials that vanish on $\mathbf{V}(I)$.

(11.a) $\mathbf{V}(\frac{y}{4} - x^2)$

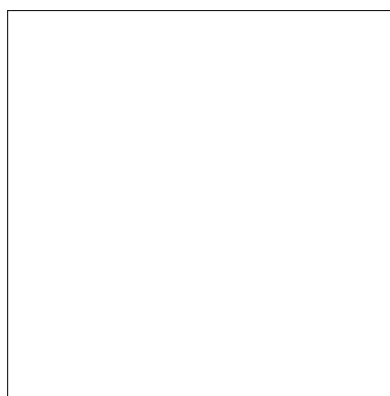
(0, 0)



(11.b) The positive half-line

(-1, 0)

(1, 0)

(11.c) $\mathbf{V}(y, x^2 - 1)$

(11.d) A square

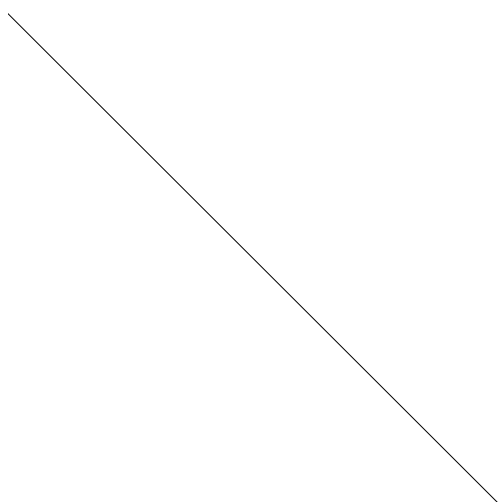
(11.e) $\mathbf{V}(x + y)$ (11.f) The sequence $(\frac{1}{n})_{n=1}^{\infty}$.

Figure 11: Three varieties on the left and three non-varieties on the right.

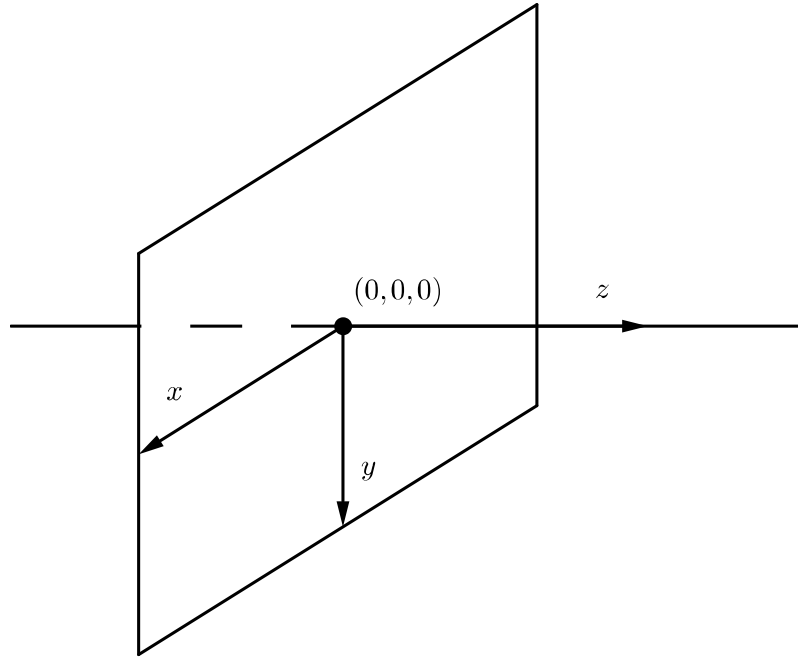


Figure 12: The variety $\mathbf{V}(xz, yz)$ consists of two irreducible components.

Theorem 2.6 (Strong Nullstellensatz [4, Theorem 4.2.6]). *Let \mathbb{k} be an algebraically closed field. If I is an ideal in $\mathbb{k}[x_1, \dots, x_n]$ then*

$$\mathbf{I}(\mathbf{V}(I)) = \sqrt{I}.$$

As a result there is a one-to-one correspondence between radical ideals and varieties, the maps \mathbf{V} : radical ideals \rightarrow varieties and \mathbf{I} : varieties \rightarrow radical ideals are inclusion-reversing inverses to each other.

The Nullstellensatz is one reason to pass to \mathbb{C} rather than working over \mathbb{R} ; when we start out with an ideal I it may be hard to determine the ideal $\mathbf{I}(\mathbf{V}(I))$ of polynomials vanishing on the variety $\mathbf{V}(I)$ defined by I . Knowing that all such polynomials lie in the radical \sqrt{I} can make proofs easier, as happens in the proof of Lemma 2.8 that $\mathbf{V}(I : J^\infty) = \overline{\mathbf{V}(I) \setminus \mathbf{V}(J)}$. Another benefit is that there are algorithms available to compute the radical of an ideal.

Some varieties are simpler than others. Let f and g define two distinct varieties $\mathbf{V}(f)$ and $\mathbf{V}(g)$. As the product fg vanishes there where at least one of the polynomials f or g vanish, the variety $\mathbf{V}(fg)$ is the union of the two subvarieties $\mathbf{V}(f)$ and $\mathbf{V}(g)$.

Whenever a variety V admits a decomposition $V = W \cup Z$ into two proper subvarieties, V is said to be reducible. Otherwise V is *irreducible*. The reducible variety $\mathbf{V}(xz, yz) \subset \mathbb{k}^3$, depicted in Figure 12, is the union of two irreducible components: the z -axis and the xy -planes.

As each point is itself a variety, any non-finite variety has an infinite amount of subvarieties. However, we can decompose a variety into a finite number of irreducible components. The following proof is a mixture of several results from Cox [4, Section 4.6]. It can be cast in the theory of primary decompositions, see Eisenbud [6, Theorem 3.1a]) for a more comprehensive treatment.

Lemma 2.7. *Any variety $V \subset \mathbb{k}^n$ can be written as a finite union $V = V_1 \cup \dots \cup V_r$ of irreducible components such that $V_i \not\subset V_j$ for any pair i and j .*

Proof. Suppose V can not be written as a finite union of irreducible varieties. In particular V is reducible, so there exist distinct proper subvarieties Z_1 and W_1 such that $V = Z_1 \cup W_1$. We can assume that Z_1 can not be written as a finite union of irreducible varieties either, so then $Z_1 = Z_2 \cup W_2$ is reducible. Repeating this process we get a chain $V \supsetneq Z_1 \supsetneq Z_2 \supsetneq \dots$ of strictly decreasing varieties. By passing to the ideals of these varieties we get an increasing chain of ideals $\mathbf{I}(V) \subset \mathbf{I}(Z_1) \subset \mathbf{I}(Z_2) \subset \dots$, as all polynomials that vanish on Z_i certainly vanish on Z_{i+1} . As $\mathbb{k}[x_1, \dots, x_n]$ is Noetherian, these ideals stabilize, and since $\mathbf{V}(\mathbf{I}(Z_i)) = Z_i$ we observe that the chain $V \supset Z_1 \supset Z_2 \supset \dots$ stabilizes as well. This contradicts the assumption that V can not be written as a finite union of irreducible varieties.

We conclude that V is a finite union $V = V_1 \cup \dots \cup V_r$ of irreducible subvarieties. If $V_i \subset V_j$ we can drop V_i from the union, proving the statement of the lemma. \square

The difference of two varieties in general is no longer a variety. Consider the case of a line L in the plane and a point p contained in L . Suppose a polynomial f vanishes on $L \setminus \{p\}$, the restriction of f to L defines a univariate polynomial with an infinite amount of zeros. By the fundamental theorem of algebra a nonzero polynomial of degree m has at most m roots, so the restriction of f to L must be the zero polynomial. But then it also vanishes on p , so the smallest variety containing $L \setminus \{p\}$ is L .

There is a relation between the smallest variety that contains the difference of two varieties defined by ideals I and J , and the variety of the colon ideal $I : J$. Over any field it is true that $\mathbf{V}(I : J) \supset \overline{\mathbf{V}(I) \setminus \mathbf{V}(J)}$. Equality holds if in addition the field is algebraically closed and I is radical [4, Theorem 4.4.7]. If \mathbb{k} is algebraically closed but we can not guarantee that I is radical, the following lemma shows we can instead pass to the saturation $I : J^\infty$.

Lemma 2.8. *Let \mathbb{k} be an algebraically closed field and let $I, J \subset \mathbb{k}[x_1, \dots, x_n]$ be ideals. Then*

$$\mathbf{V}(I : J^\infty) = \overline{\mathbf{V}(I) \setminus \mathbf{V}(J)}.$$

Proof. Let $f \in I : J^\infty$, that is, for every $j \in J$ the product fj^k is an element of I , for some $k \in \mathbb{N}$. Since for every $x \in \mathbf{V}(I) \setminus \mathbf{V}(J)$ there is a $j \in J$ that is nonzero at x , the condition $fj^k \in I$ implies that $f(x) = 0$, as $\mathbf{V}(I)$ is per definition the set of points where *all* elements of I vanish. Thus every element of $I : J^\infty$ vanishes on $\mathbf{V}(I) \setminus \mathbf{V}(J)$. Since $\overline{\mathbf{V}(I) \setminus \mathbf{V}(J)}$ is the smallest variety containing $\mathbf{V}(I) \setminus \mathbf{V}(J)$, we have shown the inclusion $\mathbf{V}(I : J^\infty) \supset \overline{\mathbf{V}(I) \setminus \mathbf{V}(J)}$.

For the reverse inclusion, let $f \in \mathbf{I}(\mathbf{V}(I) \setminus \mathbf{V}(J))$. For any $j \in J$ the product fj vanishes on the entirety of $\mathbf{V}(I)$ as j vanishes on $\mathbf{V}(J)$ and f vanishes on the complement of $\mathbf{V}(J)$ in $\mathbf{V}(I)$. Since we assumed that \mathbb{k} is algebraically closed, it follows that $fj \in \sqrt{I}$ and thus $(fj)^k \in I$ for some integer k . If $f^k j^k \in I$ for all j we can conclude that $f^k \in I : J^\infty$. We will use the fact that J is finitely generated to argue that there is indeed an integer k such that $f^k j^k \in I$ for all $j \in J$.

Let j_1, \dots, j_s be a finite set of generators for J . By the reasoning in the previous paragraph, $(fj_i)^{k_i} \in I$ for some $k_i \in \mathbb{N}$. Let k be the minimal integer such that $(fj_i)^k \in I$ for all $i \in \{1, \dots, s\}$. Let $j = \sum_{i=1}^s h_i j_i$ be an arbitrary element of J , then

$$(fj)^{ks} = \sum_{|\alpha|=ks} g_\alpha f^{ks} j_1^{\alpha_1} \dots j_s^{\alpha_s},$$

where the g_α are products of the h_i and multinomial coefficients. For each term $g_\alpha f^{ks} j_1^{\alpha_1} \dots j_s^{\alpha_s}$ at least one of the $\alpha_i \geq k$, otherwise $|\alpha| < ks$. As $f^{ks} j_1^{\alpha_1} \dots j_s^{\alpha_s}$ is a multiple of $f^k j_i^{\alpha_i}$, which is an element of I by construction, the product $(fj)^{ks}$ is a sum of elements of I and thus an element of I itself.

Thus $f^{ks} \in I : J^\infty$ as j was arbitrary. We have shown that every polynomial f that vanishes on $\mathbf{V}(I) \setminus \mathbf{V}(J)$ is present to some power in $I : J^\infty$, thus the radical $\sqrt{I : J^\infty}$ contains $\mathbf{I}(\mathbf{V}(I) \setminus \mathbf{V}(J))$ and we get the reverse inclusion $\mathbf{V}(I : J^\infty) \subset \mathbf{V}(I) \setminus \mathbf{V}(J)$. \square

A formal definition of dimension of a variety requires some work, see Chapter 9 “The Dimension of a Variety” of Cox [4]. For this thesis our intuition that points, curves and surfaces are respectively of dimensions zero, one and two will suffice to reason about dimensionality. Experimental computations of dimensions will rely on the **dim** command provided by Macaulay2.

3 Problem formulation

Toeplitz’s conjecture asks whether every Jordan curve inscribes a square. This existence question has eluded a complete answer for over a hundred years; the class of continuous curves contains rather pathological specimens.

In the algebraic square peg problem we consider algebraic plane curves rather than Jordan curves; what can we say about the set of squares inscribed on an algebraic plane curve? A straight line does not inscribe any squares, whereas a circle inscribes an uncountable amount of squares. In this thesis our aim is to count the number of inscribed squares that do not come in infinite families, a circle inscribes zero “finite” squares.

With a suitable concept of a square, the set of inscribed squares has the structure of a variety. We will see in Section 4 on page 21 that we can use Bernshtein’s Theorem to bound the size of the finite part of this variety. Before we state how many squares one can maximally inscribe, let us consider the variety of inscribed squares in some more detail. The first issue we should address is settling on a notion

of a square that is compatible with our algebraic worldview. Figure 13 is the picture to keep in mind.

Let $f \in \mathbb{R}[x, y]$ define an algebraic plane curve $\mathbf{V}_{\mathbb{R}}(f) = \{(x, y) \in \mathbb{R}^2 \mid f(x, y) = 0\}$. If we parametrize a square by a center (a, b) and an offset (c, d) to a distinguished corner, then the variety $\mathbf{V}_{\mathbb{R}}(f(a+c, b+d), f(a-c, b-d), f(a+d, b-c), f(a-d, b+c)) \subset \mathbb{R}^4$ captures all the squares inscribed on $\mathbf{V}(f)$. We consider this variety as the real part of a complex variety defined by the same algebraic relations. These relations motivate our definition of a complex square.

Definition 2 (Parametrization of a complex square). *A 4-tuple $(a, b, c, d) \in \mathbb{C}^4$ parametrizes a complex square with center (a, b) and corners $(a + c, b + d), (a + d, b - c), (a - c, b - d), (a - d, b + c)$, depicted in Figure 13. As there are four choices of (c, d) corresponding to distinguishing a particular corner, there is a four-to-one correspondence between 4-tuples and complex squares with distinct corners.*

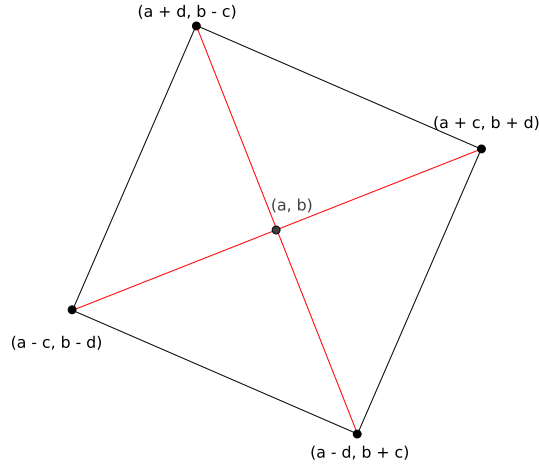


Figure 13: Center (a, b) and offset (c, d) to a distinguished corner $(a + c, b + d)$ parametrize a complex square.

When constrained to $\mathbb{R}^2 \subset \mathbb{C}^2$ this definition reduces to the familiar definition of a square: the diagonals are two perpendicular line segments of equal length intersecting each other in their midpoints. The four corners of a square are distinct as long as $(c, d) \neq (0, 0)$. If $(c, d) = (0, 0)$ the resulting square is *degenerate*, it has collapsed to a single point. We combine the definition of a complex square with a polynomial defining a plane curve to investigate the set of squares inscribed on that curve.

Let $f \in \mathbb{C}[x, y]$ define an algebraic plane curve $\mathbf{V}(f) \subset \mathbb{C}^2$. The *corner ideal* I_f of f is the ideal generated by the four polynomials that result from evaluating f at the four corners of a complex square,

$$I_f = \langle f(a + c, b + d), f(a + d, b - c), f(a - c, b - d), f(a - d, b + c) \rangle \subset \mathbb{C}[a, b, c, d].$$

The variety $\mathbf{V}(I_f)$ encodes all the squares inscribed on $\mathbf{V}(f)$, both degenerate and non-degenerate squares. All of the degenerate squares are contained in the part of

$\mathbf{V}(I_f)$ where the c and d coordinates are both zero. There is one degenerate square $(a, b, 0, 0) \in \mathbf{V}(I_f)$ for every point $(a, b) \in \mathbf{V}(f)$. Thus we identify the degenerate squares $\mathbf{V}(I_f) \cap \{c = d = 0\}$ with the original plane curve $\mathbf{V}(f)$. In the complement $\mathbf{V}(I_f) \setminus \mathbf{V}(f)$ all squares are non-degenerate.

There might be positive-dimensional components of $\mathbf{V}(I_f)$ other than the one containing $\mathbf{V}(f)$; consider a plane curve consisting of two parallel lines. The non-degenerate squares inscribed on such a curve have two vertices on each component of the curve and are centered on a third line parallel to these two components. The sidelengths of the squares equal the distance between the two parallel lines.

In this thesis we are mainly interested in counting the number of inscribed squares that lie in the zero-dimensional parts of $\mathbf{V}(I_f)$. Such squares are *isolated* as they lie in a neighbourhood that contains no other squares inscribed on $\mathbf{V}(f)$. Our main result is the following theorem, proven in the next section.

Theorem 4.8. *Let $f \in \mathbb{C}[x, y]$ of degree m define an algebraic plane curve $\mathbf{V}(f) \subset \mathbb{C}^2$. The number of isolated squares inscribed on $\mathbf{V}(f)$ is at most $(m^4 - 5m^2 - 4m)/4$.*

4 An upper bound on the number of isolated squares

The variety $\mathbf{V}(I_f)$ of squares inscribed on an algebraic plane curve $\mathbf{V}(f)$ consists of a finite number of irreducible components and hence contains a finite number of isolated points by Lemma 2.7. How do we count or estimate the number of these isolated points? We will state and use a theorem by Bernshtein to provide an upper bound on the isolated squares inscribed on an algebraic plane curve.

A classical result from algebraic geometry, called Bézout's Theorem, supplies a bound on the cardinality of a variety in terms of the degrees of the defining polynomials: If $\mathbf{V}(f_1, \dots, f_s)$ is finite, then its cardinality is at most the product $\prod \deg f_i$ of the degrees of the defining polynomials. The four generators of $I_f = \langle f(a+c, b+d), f(a+d, b-c), f(a-c, b-d), f(a-d, b+c) \rangle$ all have the same degree as f , say m . Ignoring for a moment the technicality that $\mathbf{V}(I_f)$ is not finite, from Bézout we would expect that $\mathbf{V}(I_f)$ contains at most m^4 points.

Bézout's Theorem is best stated in the context of projective space, and considering intersection multiplicities, see Cox [4, Section 8.7]. Apart from being a very useful theoretical tool, Bézout's bound acts as a baseline against which we can judge other root counting methods.

A more refined estimate than Bézout's bound makes use of more structure of the polynomials defining a variety than just their degrees. Bernshtein in his paper "The number of roots of a system of equations" [1], and Kushnirenko and Khovanskii in related papers, developed theorems to count the number of isolated roots of a polynomial system by exploiting the sparsity structure of the monomials appearing in the defining polynomials. In deference to all three mathematicians, the resulting bound is often called the BKK-bound.

Theorem 4.1 (Bernshtein[1, 3, 12, 20]). *Let $f_1, \dots, f_n \in \mathbb{C}[x_1, \dots, x_n]$. Then the number of isolated zeros in $\mathbf{V}(f_1, \dots, f_n) \cap (\mathbb{C} \setminus \{0\})^n$ is bounded from above by the mixed volume $MV(\mathcal{N}(f_1), \dots, \mathcal{N}(f_n))$ of the Newton polytopes of the generators f_i .*

A priori Bernshtein's Theorem has two drawbacks: it provides no information about positive-dimensional components of $\mathbf{V}(I_f)$, and it may miss isolated solutions that lie in a coordinate hyperplane, a linear subspace where one or more coordinates are zero. We relegate the study of the positive-dimensional components to future work.

We will argue that the interference of the coordinate hyperplanes turns out to not be a restriction for counting the zero-dimensional part of $\mathbf{V}(I_f)$; let f be a plane curve and suppose one of the isolated points p of $\mathbf{V}(I_f)$ lies in a coordinate hyperplane. Two phenomena can cause p to lie in a coordinate hyperplane: the square inscribed by $\mathbf{V}(f)$ corresponding to p either has

1. a center located on the union of the x - and y -axes $\mathbf{V}(xy)$, or
2. corners lying on the translate $\mathbf{V}((x-a)(y-b))$ of the coordinate-axes to its center.

Note that both phenomena can occur at the same time, Figure 14 depicts the square $(0, 0, 0, 1)$ inscribed by $\mathbf{V}(xy)$.

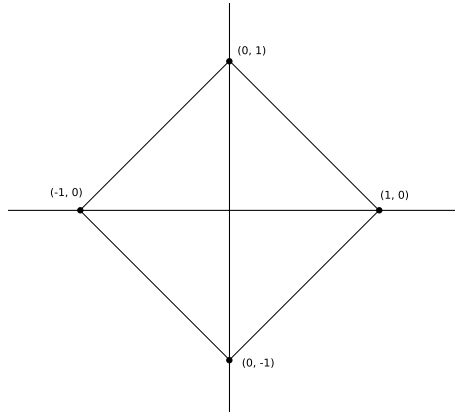


Figure 14: The square $(0, 0, 0, 1)$ lies in three coordinate hyperplanes.

Both these situations are an artifact of choosing coordinates for the geometric object that is the curve. By translating the curve we can ensure the center of the square corresponding to p no longer lies on $\mathbf{V}(xy)$. A rotation suffices to ensure the corners and the center do not lie on the same translate of $\mathbf{V}(xy)$.

As $\mathbf{V}(I_f)$ has a finite number of irreducible components, there exists a curve f' obtainable from f by translations and rotations so that none of the zero-dimensional components of $\mathbf{V}(I_{f'})$ lie in a coordinate hyperplane. For the purpose of counting the number of isolated squares inscribed on a curve we can safely assume Bernshtein's Theorem accounts for all of them.

We want to bound the number of isolated squares in $\mathbf{V}(I_f)$ using Bernshtein's Theorem; What are the concrete objects appearing in the expression for the mixed volume $MV(\mathcal{N}(f_1), \mathcal{N}(f_2), \mathcal{N}(f_3), \mathcal{N}(f_4))$ for the algebraic square peg problem? It is straightforward to calculate the mixed volume for the polynomials of the form $f(a+c, b+d)$ that generate $I_f = \langle f(a+c, b+d), f(a+d, b-c), f(a-c, b-d), f(a-d, b+c) \rangle$, but we show in Section 4.1 that these generators do not provide a useful BKK bound in general.

We pursue a five step program to obtain the bound $(m^4 - 5m^2 + 4m)/4$ on the number of isolated squares inscribed on an algebraic plane curve of degree m . The first step is a better choice of generators g_i of I_f in Section 4.2 on the next page. In Section 4.3 on the following page we will see that this choice will allow for more control on the monomials present in the generators. That control translates into smaller Newton polytopes in the third step discussed in Section 4.4 on page 27. The Minkowski sum of these smaller Newton polytopes is described in Section 4.5 on page 31. In the fifth and final step of our program we calculate the volume of the Minkowski sum $\sum \lambda_i \mathcal{N}(g_i)$ and extract the mixed volume of the $\mathcal{N}(g_i)$.

The fact that an algebraic plane curve of degree m inscribes at most $(m^4 - 5m^2 + 4m)/4$ isolated squares is then an immediate consequence of invoking Bernshtein's Theorem, Theorem 4.1, with the data $MV(\mathcal{N}(g_1), \mathcal{N}(g_2), \mathcal{N}(g_3), \mathcal{N}(g_4))$ as calculated by the five step program.

4.1 The effect of naive generators

Let $f = \sum c_{i,j} x^i y^j$ of degree m define a plane curve. We saw that an application of Bézout's Theorem to $I_f = \langle f(a+c, b+d), f(a+d, b-c), f(a-c, b-d), f(a-d, b+c) \rangle$ only tells us that the finite part of $\mathbf{V}(I_f)$ is at most of size m^4 . An application of Bernshtein's Theorem will bound the number of isolated squares inscribed on $\mathbf{V}(f)$, up to the squares that lie in a coordinate hyperplane. Can we do better than Bézout's bound by applying Bernshtein's Theorem? Unfortunately, not immediately.

Suppose that the monomials 1 , x^m and y^m appear in f with nonzero coefficients, that is, the Newton polytope of f is as large as it can be for a curve of degree m . To calculate the BKK bound we first determine what the Newton polytopes of $f(a+c, b+d)$, $f(a-c, b-d)$, $f(a+d, b-c)$, and $f(a-d, b+c)$ are by looking at the monomials occuring in them.

Substituting the corner $(a-c, b-d)$ into f and expanding $f(a-c, b-d)$, the monomial x^m gets mapped to $\sum_{j=0}^m \binom{m}{j} a^j (-1)^{m-j} c^{m-j}$, which establishes that a^m and c^m appear with nonzero coefficients in $f(a-c, b-d)$. Similar reasoning applied to y^m guarantees the presence of the monomials b^m and d^m . As presence of the monomial 1 is unaffected by the substitution, we see that the Newton polytope $\mathcal{N}(f(a-c, b-d))$ contains at least $\text{conv}\{a^m, b^m, c^m, d^m, 1\} = m\text{conv}\{0, e_1, e_2, e_3, e_4\} = m\Delta$. All monomials of degree at most m are contained in $m\Delta$, so we conclude that $\mathcal{N}(f(a-c, b-d)) = m\Delta$. The same argument goes through for the other Newton

polytopes. Calculating the volume of the Minkowski sum $\sum_1^4 \lambda_i m\Delta$ we see that

$$\text{Vol}_4 \left(\sum_1^4 \lambda_i m\Delta \right) = \left(\sum_1^4 \lambda_i \right)^n \text{Vol}_4(m\Delta),$$

so the mixed volume of the Newton polytopes is $4!$ times the volume of $m\Delta$. That is, $4!m^4/4! = m^4$.

The resulting estimate is the same as the one supplied by Bézout. To overcome this problem it is necessary that we pick a set of generators for I_f whose Newton polytopes are smaller than $m\Delta$. This is the first step of our five step program, which we undertake in Section 4.2.

4.2 A better choice of generators

The issue with the naive generators of $I_f = \langle f(a+c, b+d), f(a+d, b-c), f(a-c, b-d), f(a-d, b+c) \rangle$ not providing a BKK bound different from Bézout's bound is that they contain a lot of redundant information. By reducing the redundancy in the generators of I_f we get a set of generators for which we will be able to show in the next two sections that their Newton polytopes are smaller than those of the original generators.

Define polynomials g_1, g_2, g_3, g_4 by

$$\begin{aligned} g_1 &= f(a+c, b+d) + f(a-c, b-d) - f(a-d, b+c) - f(a+d, b-c), \\ g_2 &= f(a+c, b+d) - f(a-c, b-d), \\ g_3 &= f(a-d, b+c) - f(a+d, b-c), \\ g_4 &= f(a+d, b-c). \end{aligned} \tag{1}$$

As the g_i are linear combinations of the generators of I_f , it is clear that they generate a subideal of I_f . It is easily checked that the original generators are contained in this subideal as well, so $\langle g_1, g_2, g_3, g_4 \rangle = \langle f(a+c, b+d), f(a+d, b-c), f(a-c, b-d), f(a-d, b+c) \rangle$. It may not be immediately clear that we have gained anything by this different choice of generators. Over the course of Section 4.3, Section 4.4 on page 27, Section 4.5 on page 31 and Section 4.6 on page 33 we will show that $MV(\mathcal{N}(g_1), \mathcal{N}(g_2), \mathcal{N}(g_3), \mathcal{N}(g_4)) = m^4 - 5m^2 + 4m$, a definite improvement over the previous estimate m^4 .

4.3 Monomials present in g_i

We have shown that the Newton polytopes $\mathcal{N}(f(a+c, b+d))$ of the generators of I_f all equal the simplex $m\Delta$ by showing that they contain the vertices $(0, 0, 0, 0)$ and me_i for $i = 1, 2, 3, 4$. Since $g_4 = f(a+d, b-c)$ we know that $\mathcal{N}(g_4) = m\Delta$.

The construction of the generators g_1, g_2 , and g_3 causes the constant term to disappear, but it is less clear which monomials of the g_i then will be vertices of the Newton polytopes. Which monomials are even present in the generators g_i ?

Since our five step program has the aim of proving the bound $(m^4 - 5m^2 + 4m)/4$ for all curves of degree m , we can assume that the coefficients of $f = \sum_{i+j \leq m} C_{i,j} x^i y^j$

are not related in such a way that they cause cancellation in the g_i . After some algebraic manipulation we will see that the presence of $a^{\gamma_1}b^{\gamma_2}c^{\gamma_3}d^{\gamma_4}$ in g_i then only depends on i and the parity of $\gamma_3 + \gamma_4$, barring the exceptional case for g_1 whenever $\gamma_3 = \gamma_4$ is an even number. The presence of the monomial $a^{\gamma_1}b^{\gamma_2}c^{\gamma_3}d^{\gamma_4}$ in g_i can be read off from Equation (2) on the following page and is summarized in Table 1. An example of the monomials present in a fourth degree curve is displayed in Section 4.3.1 on the following page.

	$\gamma_3 + \gamma_4$ odd	$\gamma_3 + \gamma_4$ even	
		$\gamma_3 = \gamma_4$, even	otherwise
g_1	absent	absent	present
g_2 and g_3	present	absent	absent
g_4	present	present	present

Table 1: Presence of monomials $a^{\gamma_1}b^{\gamma_2}c^{\gamma_3}d^{\gamma_4}$ in g_i depends on the parity of $\gamma_3 + \gamma_4$.

Substituting the expressions for the corners into the variables x and y transforms monomials $x^i y^j$ of degree k to monomials $a^{\gamma_1}b^{\gamma_2}c^{\gamma_3}d^{\gamma_4}$ of the same degree k , as seen from the binomial expansion

$$(a + c)^i(b + d)^j = \sum_{p=0}^i \binom{i}{p} a^p c^{i-p} \sum_{q=0}^j \binom{j}{q} b^q d^{j-q}.$$

To establish the presence or absence of monomials in g_i of degree k it thus suffices to consider the k -th homogeneous part of f . We consider $(g_i)_k = h_{i1}f(a + c, b + d)_k + h_{i2}f(a - c, b - d)_k + h_{i3}f(a - d, b + c)_k + h_{i4}f(a + d, b - c)_k$, where $h_{ij} \in \{-1, 0, 1\}$ according to the choices in Equation (1) on the previous page. Expanding the definitions results in the equations

$$\begin{aligned} f(a \pm c, b \pm d)_k &= \sum_{j=0}^k C_{k-j,j} (a \pm c)^{k-j} (b \pm d)^j, \\ f(a \pm d, b \mp c)_k &= \sum_{j=0}^k C_{k-j,j} (a \pm d)^{k-j} (b \mp c)^j. \end{aligned}$$

In addition to expanding the binomial terms $(a \pm d)^{k-j}$ and $(b \mp c)^j$ in $f(a \pm d, b \mp c)_k$ as before, we keep track of the coefficients $C_{k-j,j}$ and minus signs. Gathering monomials we get

$$\begin{aligned} f(a \pm d, b \mp c)_k &= \sum_{j=0}^k C_{k-j,j} \sum_{i=0}^{k-j} \binom{k-j}{i} a^i d^{k-j-i} (\pm)^{k-j-i} \sum_{l=0}^j \binom{j}{l} b^l c^{j-l} (\mp)^{j-l} \\ &= \sum_{j=0}^k \sum_{i=0}^{k-j} \sum_{l=0}^j C_{k-j,j} \binom{k-j}{i} \binom{j}{l} (\pm)^{k-j-i} (\mp)^{j-l} a^i b^l c^{j-l} d^{k-j-i}. \end{aligned}$$

Summing up $h_{i3}f(a - d, b + c) + h_{i4}f(a + d, b - c)$ we can read off the coefficient of the monomial with exponent $\gamma = (i, l, j - l, k - j - i)$ as

$$C_{\gamma_1+\gamma_4, \gamma_2+\gamma_3} \binom{\gamma_1 + \gamma_4}{\gamma_1} \binom{\gamma_2 + \gamma_3}{\gamma_2} (h_{i3}(-1)^{\gamma_4} + h_{i4}(-1)^{\gamma_3}).$$

The derivation for $h_{i1}f(a+c, b+d) + h_{i2}f(a-c, b-d)$ is analogous. The constant term $C_{0,0}$ disappears from g_i as long as the sum $h_{i1} + h_{i2} + h_{i3} + h_{i4}$ vanishes. With our choice of generators this is the case. For $k > 0$ the degree k monomial $a^{\gamma_1}b^{\gamma_2}c^{\gamma_3}d^{\gamma_4}$ occurs in g_i in the term

$$\left[\binom{\gamma_1 + \gamma_3}{\gamma_1} \binom{\gamma_2 + \gamma_4}{\gamma_2} C_{\gamma_1 + \gamma_3, \gamma_2 + \gamma_4} (h_{i1} + h_{i2}(-1)^{\gamma_3 + \gamma_4}) + \binom{\gamma_1 + \gamma_4}{\gamma_1} \binom{\gamma_2 + \gamma_3}{\gamma_2} C_{\gamma_1 + \gamma_4, \gamma_2 + \gamma_3} (h_{i3}(-1)^{\gamma_4} + h_{i4}(-1)^{\gamma_3}) \right] a^{\gamma_1}b^{\gamma_2}c^{\gamma_3}d^{\gamma_4}. \quad (2)$$

Here we see that for particular values of the coefficients C_α some extra cancellation may occur that does not happen in the general case. However, for a generic choice of coefficients, if $\gamma_3 \neq \gamma_4$ the two summands between brackets in Equation (2) are independent. Both g_2 and g_3 have two of the h_{ij} set to zero, so then the bracketed term is zero if, respectively,

$$1 + (-1)(-1)^{\gamma_3 + \gamma_4} = 0, \quad \text{or} \quad (-1)^{\gamma_4} + (-1)(-1)^{\gamma_3} = 0.$$

Multiplying the second equation with $(-1)^{\gamma_3}$ we obtain the equation $(-1)^{\gamma_3 + \gamma_4} - 1 = 0$. Thus for both g_2 and g_3 if $\gamma_3 + \gamma_4$ is even the monomial $a^{\gamma_1}b^{\gamma_2}c^{\gamma_3}d^{\gamma_4}$ is absent, otherwise it is present.

A similar argument for g_1 shows that $a^{\gamma_1}b^{\gamma_2}c^{\gamma_3}d^{\gamma_4}$ is absent from g_1 if $\gamma_3 + \gamma_4$ is odd, since $h_{11} = h_{12}$ and $h_{13} = h_{14}$. When $\gamma_3 + \gamma_4$ is even there are two further cases to distinguish; when $\gamma_3 = \gamma_4$ is an even number, Equation (2) collapses to

$$\binom{\gamma_1 + \gamma_3}{\gamma_1} \binom{\gamma_2 + \gamma_4}{\gamma_2} C_{\gamma_1 + \gamma_3, \gamma_2 + \gamma_4} (1 + 1 - 1 - 1) a^{\gamma_1}b^{\gamma_2}c^{\gamma_3}d^{\gamma_4} = 0.$$

Otherwise, either $\gamma_3 = \gamma_4$ is odd and Equation (2) evaluates to

$$4 \binom{\gamma_1 + \gamma_3}{\gamma_1} \binom{\gamma_2 + \gamma_4}{\gamma_2} C_{\gamma_1 + \gamma_3, \gamma_2 + \gamma_4} a^{\gamma_1}b^{\gamma_2}c^{\gamma_3}d^{\gamma_4},$$

or $\gamma_3 \neq \gamma_4$ and the two equations $1 + (-1)^{\gamma_3 + \gamma_4} = 1$ and $(-1)(-1)^{\gamma_4} + (-1)(-1)^{\gamma_3}$ need to be simultaneously zero.

In conclusion: monomials of odd c, d -degree are present in g_2 and g_3 but absent in g_1 . Monomials of even c, d -degree are absent in g_2 and g_3 but present in g_1 when the degrees of c and d are not both even. These relations are tabulated in Table 1 on the previous page.

4.3.1 Example for a fourth degree curve

The presence of monomials in the g_i so far is a little abstract. Let us look at a somewhat more concrete example by considering a generic fourth degree curve $f = C_{4,0}x^4 + C_{3,1}x^3y + C_{2,2}x^2y^2 + C_{1,3}xy^3 + C_{0,4}y^4 + C_{3,0}x^3 + C_{2,1}x^2y + C_{1,2}xy^2 + C_{0,3}y^3 + C_{2,0}x^2 + C_{1,1}xy + C_{0,2}y^2 + C_{1,0}x + C_{0,1}y + C_{0,0}$. According to Table 1, the

monomials in g_1 should be all even c, d -degree monomials of total degree at most four, excluding the monomials 1 and c^2d^2 , which is indeed the case:

$$\begin{aligned} g_1 = & (-2C_{2,2} + 12C_{4,0})a^2c^2 + (-6C_{1,3} + 6C_{3,1})abc^2 + (-12C_{0,4} + 2C_{2,2})b^2c^2 \\ & + (-2C_{0,4} + 2C_{4,0})c^4 + 12C_{3,1}a^2cd + 16C_{2,2}abcd + 12C_{1,3}b^2cd \\ & + (2C_{1,3} + 2C_{3,1})c^3d + (2C_{2,2} - 12C_{4,0})a^2d^2 + (6C_{1,3} - 6C_{3,1})abd^2 \\ & + (12C_{0,4} - 2C_{2,2})b^2d^2 + (2C_{1,3} + 2C_{3,1})cd^3 + (2C_{0,4} - 2C_{4,0})d^4 \\ & + (-2C_{1,2} + 6C_{3,0})ac^2 + (2C_{2,1} - 6C_{0,3})bc^2 + 8C_{2,1}acd + 8C_{1,2}bcd \\ & + (2C_{1,2} - 6C_{3,0})ad^2 + (-2C_{2,1} + 6C_{0,3})bd^2 + (2C_{2,0} - 2C_{0,2})c^2 \\ & + 4C_{1,1}cd + (-2C_{2,0} + 2C_{0,2})d^2. \end{aligned}$$

Of the list of monomials $\{a^2c^2, abc^2, b^2c^2, c^4, a^2cd, abcd, b^2cd, c^3d, a^2d^2, abd^2, b^2d^2, cd^3, d^4, ac^2, bc^2, acd, bcd, ad^2, bd^2, c^2, cd, d^2\}$ occuring in g_1 , those with only the variables c and d are depicted in Figure 15.

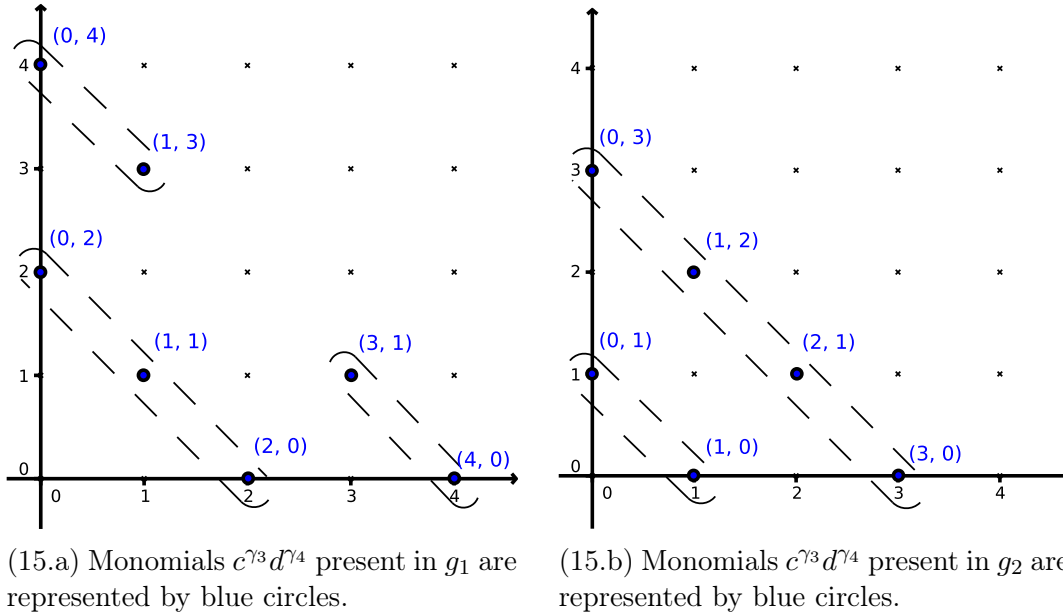


Figure 15: The parity of $\gamma_3 + \gamma_4$ determines whether monomials $c^{\gamma_3}d^{\gamma_4}$ are present in the generators g_1 and g_2 .

4.4 Newton polytope shapes

In the previous two sections we have shown which monomials are present in the g_i . In the third step of our five step program to prove that the mixed volume $MV(\mathcal{N}(g_1), \mathcal{N}(g_2), \mathcal{N}(g_3), \mathcal{N}(g_4)) = m^4 - 5m^2 + 4m$ we describe the Newton polytopes $\mathcal{N}(g_i)$. We already know that $\mathcal{N}(g_4) = m\Delta$ and $\mathcal{N}(g_i) \subset m\Delta$ since the g_i are of degree m . We also saw from Table 1 on page 25 that $\mathcal{N}(g_2) = \mathcal{N}(g_3)$.

In this section we prove that the Newton polytopes $\mathcal{N}(g_1)$ and $\mathcal{N}(g_2)$ alternate between the two types of simple polytopes P_1 and P_2 from Definition 3, according

to the parity of m . This dependence is summarized in Table 2. Their Schlegel diagrams are depicted in Figure 16 on the next page and Figure 17 on the following page; the vertex descriptions of P_1 and P_2 as well as expressions of the vertices as intersections of facets are given in Lemma 4.2 and Lemma 4.3.

The Newton polytopes $\mathcal{N}(g_i)$ are the convex hulls of the monomials appearing in the g_i ; the pertinent information about g_1 , g_2 and g_3 is shown in Table 1 on page 25. Let us rewrite this information in a form convenient for thinking about polytopes as intersections of halfspaces,

$$\begin{aligned}\{\text{exponents of } g_1\} &= m\Delta \cap \bigcup_{n=0}^{\infty} \{x_3 + x_4 = 2n + 2\} \setminus \{x_3 = x_4 \text{ even}\}, \\ \{\text{exponents of } g_2\} &= m\Delta \cap \bigcup_{n=0}^{\infty} \{x_3 + x_4 = 2n + 1\}.\end{aligned}$$

The extreme monomials determine the convex hull, so we can express $\mathcal{N}(g_1)$ and $\mathcal{N}(g_2)$ as the following intersections of halfspaces:

$$\begin{aligned}\mathcal{N}(g_1) &= m\Delta \cap H_{x_3+x_4 \geq 2} \cap H_{x_3+x_4 \leq 2n_1+2}, \\ \mathcal{N}(g_2) &= m\Delta \cap H_{x_3+x_4 \geq 1} \cap H_{x_3+x_4 \leq 2n_2+1},\end{aligned}$$

where n_1 and n_2 are the largest integers n_1 and n_2 such that $2n_1 + 2$ and $2n_2 + 1$ are both smaller than or equal to m . If m is even, then the halfspace $H_{x_3+x_4 \leq 2n_1+2}$ is redundant as the hyperplane $H_{x_3+x_4=2n_1+2}$ intersects $m\Delta$ in the facet defined by the hyperplane $H_{\sum x_i=m}$. When m is odd, $H_{x_3+x_4 \leq 2n_2+1}$ is redundant. These polytopes are central to the rest of this section, so let us fix some notation.

Definition 3. *The three types of polytopes P_0 , P_1 and P_2 are obtained from $m\Delta$ by successively adding a facet-defining hyperplane parallel to $H_{(0,0,1,1)}$ so that*

$$\begin{aligned}P_0 &= P_0(m) = m\Delta, \\ P_1 &= P_1(m, l) = P_0 \cap H_{x_3+x_4 \geq l}, \\ P_2 &= P_2(m, l, k) = P_1(m, l) \cap H_{x_3+x_4 \leq k}.\end{aligned}$$

The polytopes P_1 and P_2 are both four-dimensional when $m \geq 4$ but not for $m \in \{2, 3\}$. Schlegel diagrams for $m = 4$ are depicted in Figure 16 on the following page and Figure 17 on the next page. With the notation from Definition 3 we can summarize the Newton polytopes of g_1 and g_2 for even and odd m as

	$m = 2n + 2$	$m = 2n + 1$
$\mathcal{N}(g_1)$	$P_1(m, 2)$	$P_2(m, 2, m - 1)$
$\mathcal{N}(g_2)$	$P_2(m, 1, m - 1)$	$P_1(m, 1).$

Table 2: $\mathcal{N}(g_1)$ and $\mathcal{N}(g_2)$ alternate between the polytopes P_1 and P_2

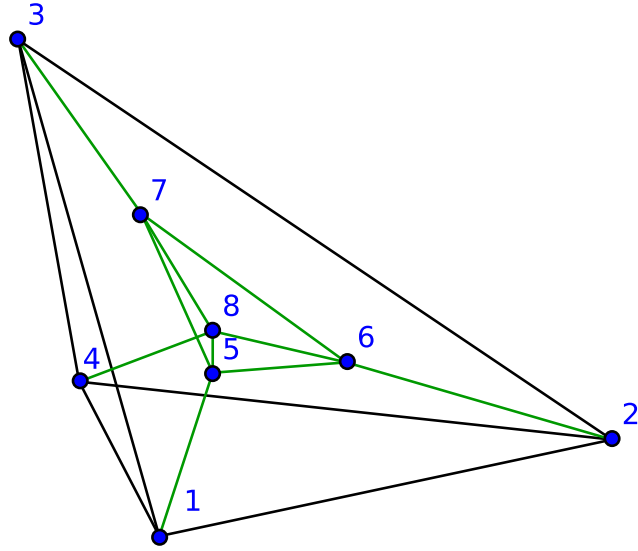


Figure 16: Schlegel diagram of P_1 projected onto its facet where $x_4 = 0$.

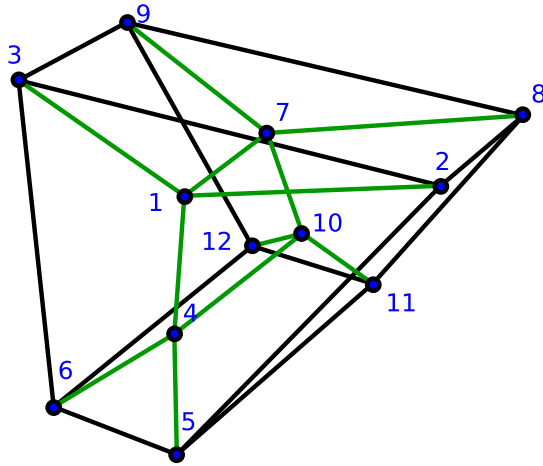


Figure 17: Schlegel diagram of P_2 projected onto its facet where $\sum x_i = m$.

The combinatorial structure of the polytopes P_1 and P_2 , that is, which vertices are included in which faces, can be read off from the Schlegel diagrams. For those unconvinced that the Schlegel diagrams are correct, the next two lemmas establish vertex descriptions and the facet-vertex incidences of $P_1(m, l)$ and $P_2(m, l, k)$, without the visual aid.

Lemma 4.2. *Let $m \geq 4$ and $0 < l < m$. Then $P_1 = P_1(m, l)$, as defined in Definition 3, is a simple polytope with eight labeled vertices given by the columns of the matrix*

$$\begin{pmatrix} 1 & 2 & 3 & 4 & 5 & 6 & 7 & 8 \\ 0 & m-l & 0 & 0 & 0 & m-l & 0 & 0 \\ 0 & 0 & m-l & 0 & 0 & 0 & m-l & 0 \\ l & l & l & m & 0 & 0 & 0 & 0 \\ 0 & 0 & 0 & 0 & l & l & l & m \end{pmatrix}.$$

The vertices are expressed as intersections of hyperplanes in the following way,

$$\begin{aligned} H_{-e_1,0} \cap H_{-e_2,0} \cap H_{-e_i,0} \cap H_{\sum e_k,m} &= \{me_j\}, \\ H_{-e_1,0} \cap H_{-e_2,0} \cap H_{-e_i,0} \cap H_{-e_3-e_4,l} &= \{le_j\}, \\ H_{-e_1+j_1,0} \cap H_{-e_3+j_2,0} \cap H_{\sum e_i,m} \cap H_{-e_3-e_4,l} &= \{(m-l)e_{2-j_1} + le_{4-j_2}\}, \end{aligned} \quad (3)$$

where $i, j \in \{3, 4\}$, $i \neq j$ and $j_1, j_2 \in \{0, 1\}$.

Proof. The polytope $P_1(m, l)$ has six facet-defining hyperplanes. There are $\binom{6}{4}$ ways to form intersections of four of these hyperplanes. Due to the constraint $x_3 + x_4 \geq l$ the intersection $H_{-e_3,0} \cap H_{-e_4,0}$ does not contain any part of P_1 . The intersection $H_{-e_1,0} \cap H_{-e_2,0} \cap H_{-e_3-e_4,l} \cap H_{\sum e_i,m}$ is empty due to conflicting constraints. Thus any intersection of five hyperplanes is either empty or lies outside P_1 , as a five-fold intersection of the hyperplanes defining P_1 involves at least one of these two intersections. Hence any vertex of P_1 is contained in at most four facets.

This leaves $2\binom{4}{3} = 8$ combinations of intersecting four hyperplanes to check, each involving exactly one of $H_{-e_3,0}$ or $H_{-e_4,0}$. These eight intersections are listed above and result in eight distinct vertices, each of which is contained in precisely four facets. \square

We obtain P_2 from P_1 by intersecting it with the halfspace $H_{x_3+x_4 \leq k}$. The facet of P_2 defined by this halfspace is parallel to the hyperplane $H_{x_3+x_4 \geq l}$ that cuts out P_1 from P_0 , and thus the derivation of P_2 follows the same kind of reasoning as Lemma 4.2.

Lemma 4.3. *Let $0 < l < k < m$ and $m \geq 4$. Then $P_2 = P_2(m, l, k)$ is a simple polytope with twelve labeled vertices given by the columns of the matrix*

$$\begin{pmatrix} 1 & 2 & 3 & 4 & 5 & 6 & 7 & 8 & 9 & 10 & 11 & 12 \\ 0 & m-l & 0 & 0 & m-k & 0 & 0 & m-l & 0 & 0 & m-k & 0 \\ 0 & 0 & m-l & 0 & 0 & m-k & 0 & 0 & m-l & 0 & 0 & m-k \\ l & l & l & k & k & k & 0 & 0 & 0 & 0 & 0 & 0 \\ 0 & 0 & 0 & 0 & 0 & 0 & l & l & l & k & k & k \end{pmatrix}.$$

The vertices are expressed as intersections of hyperplanes in the following way,

$$\begin{aligned} H_{-e_1,0} \cap H_{-e_2,0} \cap H_{e_i,0} \cap H_{e_3+e_4,k} &= \{ke_j\}, \\ H_{-e_1,0} \cap H_{-e_2,0} \cap H_{e_i,0} \cap H_{-e_3-e_4,l} &= \{le_j\}, \\ H_{-e_1+j_1,0} \cap H_{-e_3+j_2,0} \cap H_{e_3+e_4,k} \cap H_{\sum e_i,m} &= \{(m-k)e_{2-j_1} + ke_{4-j_2}\}, \\ H_{-e_1+j_1,0} \cap H_{-e_3+j_2,0} \cap H_{-e_3-e_4,l} \cap H_{\sum e_i,m} &= \{(m-l)e_{2-j_1} + le_{4-j_2}\}, \end{aligned}$$

where $i, j \in \{3, 4\}$, $i \neq j$ and $j_1, j_2 \in \{0, 1\}$.

Proof. As in the previous lemma, the intersection $H_{-e_3,0} \cap H_{-e_4,0}$ contains no part of P_2 . Likewise, the intersection $H_{-e_1,0} \cap H_{-e_2,0} \cap H_{\sum e_i,m}$ contains no vertices due to the conflicting constraint $x_3 + x_4 \leq k$. Again the implication is that no intersection of five hyperplanes contains a vertex of P_2 .

Of the four-fold intersections those involving neither of $H_{-e_3,0}$ nor $H_{-e_4,0}$ are either contained in $H_{e_3+e_4,k} \cap H_{-e_3-e_4,l}$ or in $H_{-e_1,0} \cap H_{-e_2,0} \cap H_{\sum e_i,m}$, and thus contribute nothing. The remaining $4\binom{3}{2} = 12$ options involving exactly one of $\{H_{-e_3,0}, H_{-e_4,0}\}$ and exactly one of $\{H_{e_3+e_4,k}, H_{-e_3-e_4,l}\}$ all contribute a vertex of P_2 . □

4.5 Minkowski sum shapes

We are over halfway in our five step program to proving that there are at most $(m^4 - 5m^2 + 4m)/4$ squares inscribed on an algebraic plane curve of degree m . In the previous section we showed that the Newton polytopes $\mathcal{N}(g_1)$ are of the types P_0 , P_1 and P_2 defined in Definition 3. In the fourth step of our program we show that the Minkowski sum $\lambda_1\mathcal{N}(g_1) + \lambda_2\mathcal{N}(g_2) + \lambda_3\mathcal{N}(g_3) + \lambda_4\mathcal{N}(g_4)$ is itself a P_2 type polytope. This result, Lemma 4.5, is due to the combination of two facts: the common refinement of the normal fans of P_0 , P_1 and P_2 is the normal fan of P_2 , and Lemma 4.4, which states that the normal fan of a Minkowski sum is the common refinement of the normal fans of the summands. Knowing the form of the Minkowski sum enables us to calculate its volume to finally determine the mixed volume of the $\mathcal{N}(g_i)$.

As the polytopes $\mathcal{N}(g_i)$ are of different shape depending on the parity of m , as summarized in Table 2 on page 28, we rewrite the Minkowski sum $\sum \lambda_i\mathcal{N}(g_i)$ as $\mu_1P_1 + \mu_2P_2 + \lambda_4\mathcal{N}(g_4)$. Since $\mathcal{N}(g_2) = \mathcal{N}(g_3)$ one of μ_1 or μ_2 equals $\lambda_2 + \lambda_3$, while the other coefficient μ_i is set to λ_1 . Table 3 summarizes the values of μ_1 and μ_2 .

	m even	m odd
μ_1	λ_1	$\lambda_2 + \lambda_3$
μ_2	$\lambda_2 + \lambda_3$	λ_1

Table 3: The values of the coefficients μ_1 and μ_2 in the expression of $\sum_{i=1}^4 \lambda_i\mathcal{N}(g_i) = \mu_1P_1 + \mu_2P_2 + \lambda_4\mathcal{N}(g_4)$.

The following lemma from Ziegler's Lectures on Polytopes tells us that we should look at the normal fans of the Newton polytopes to determine the normal fan of the Minkowski sum.

Lemma 4.4 ([27, Proposition 7.12, p198]). *The normal fan of a Minkowski sum is the common refinement of normal fans of the summands.*

Proof. Let $P = P_1 + \cdots + P_n$ and let Γ be a face of P . Fix a functional α in the normal cone of Γ , that is, Γ is precisely the subset of P that is maximal under α . Let $\Gamma \ni v = v_1 + \cdots + v_n$. Suppose that some v_j does not maximize α in P_i . Then there exists a $w_j \in P_j$ such that

$$\alpha(v) = \sum \alpha(v_i) < \sum_{i \neq j} \alpha(v_i) + \alpha(w_j) = \alpha(v - v_j + w_j).$$

The vector $v - v_j + w_j$ is an element of P by definition of the Minkowski sum, but this contradicts Γ being the maximizer of α . Thus the faces of the P_i that are the summands in $\Gamma = \Gamma_1 + \cdots + \Gamma_n$ are themselves maximizers of P_i with respect to α . The normal cone of Γ is then the intersection of the normal cones of the Γ_i . \square

The normal cone of any face of a polytope is spanned by the facet normals of the facets said face is contained in. Thus, the normal fan of a polytope is completely determined by the normal cones of the vertices of a polytope. The descriptions of the vertices as intersections of hyperplanes in Lemma 4.2 and Lemma 4.3 directly tell us what the normal cones of the vertices of P_1 and P_2 are. To show that $\mu_1 P_1(m, l_1) + \mu_2 P_2(m, l_2, k) + m\Delta$ is of type P_2 we first show that P_0 , P_1 and P_2 have normal fans that successively refine each other.

Lemma 4.5. *The Minkowski sum $\mu_1 P_1(m, l_1) + \mu_2 P_2(m, l_2, k) + m\Delta = P_2(m', l', k')$ where*

$$m' = (\mu_1 + \mu_2 + \lambda_4)m, \quad l' = \mu_1 l_1 + \mu_2 l_2, \quad k' = (\mu_1 + \lambda_4)m + \mu_2 k.$$

Proof. We obtain P_{i+1} from P_i by introducing an additional facet-defining hyperplane H^i . As P_i and P_{i+1} are both simple, any vertices contained in H^i are contained in three other hyperplanes. The normal cone of a vertex in H^i lies within the normal cone of a vertex of P_i cut off from P_{i+1} by H^i ; each vertex cut off lies in an intersection $H_1^i \cap \cdots \cap H_{r_i}^i$ of hyperplanes whose facet-normals generate a cone containing the facet-normal of H^i .

We see from the vertex-facet incidences of Lemma 4.2 and Lemma 4.3 that the vertices of P_0 that are cut off from P_1 by $H_{-e_3-e_4,l}$ lie in the intersection $H_{-e_3,0} \cap H_{-e_4,0}$ and the facet-normal $-e_3 - e_4$ of $H_{-e_3-e_4,l}$ is the sum of the facet-normals of $H_{-e_3,0}$ and $H_{-e_4,0}$.

Likewise, the vertices of P_2 that are cut off from P_1 by $H_{e_3+e_4,k}$ lie in the intersection $H_{-e_1,0} \cap H_{-e_2,0} \cap H_{\sum e_i,m}$ and again the facet-normal of $H_{e_3+e_4,k}$ is the sum of the facet normals $e_1 + e_2 + e_3 + e_4$, $-e_1$ and $-e_2$.

Thus the normal fan of P_2 is a refinement of the normal fan of P_1 which is a refinement of the normal fan of P_0 ; the common refinement of the normal fans of

P_0 , P_1 and P_2 then is the normal fan of P_2 . By Lemma 4.4 this is also the normal fan of the Minkowski sum $\sum_{i=1}^4 \lambda_i \mathcal{N}(g_i)$.

In particular the Minkowski sum is itself a $P_2(m', l', k')$ polytope for appropriate constants m' , l' and k' . We can read off the values of m' and k' from the vertices of $P_2(m', l', k')$ contained in the intersection of hyperplanes with normals $(0, 0, 1, 1)$ and $(1, 1, 1, 1)$, for example the vertex $(m' - k', 0, k', 0)$. This vertex is the sum of vertices v_i of the summands of $\mu_1 P_1 + \mu_2 P_2 + P_0$ that have a normal cone containing its normal cone.

As the normal cone of $H_{-e_1,0} \cap H_{-e_2,0} \cap H_{-e_3,0} \cap H_{\sum e_i, m}$ contains the normal cone of $H_{-e_1+j,0} \cap H_{-e_3,0} \cap H_{\sum e_i, m} \cap H_{e_3+e_4, k}$, we get the vertex $(\mu_1 + \lambda_4)m e_4 + \mu_2((m - k)e_{2-j} + k e_4)$. Summing up the coefficients gives $m' = (\mu_1 + \mu_2 + \lambda_4)m$. The coefficient of e_4 is $k' = (\mu_1 + \lambda_4)m + \mu_2 k$.

The value of l' can be recovered from a vertex contained in $H_{-e_3-e_4, l}$. As the normal cone of $H_{-e_1,0} \cap H_{-e_2,0} \cap H_{-e_3,0} \cap H_{-e_4,0}$ contains the normal cone of $H_{-e_1,0} \cap H_{-e_2,0} \cap H_{-e_3,0} \cap H_{-e_3-e_4, l}$, we get the vertex $(\mu_1 l_1 + \mu_2 l_2)e_4$ of the Minkowski sum, so $l' = \mu_1 l_1 + \mu_2 l_2$. \square

4.6 Minkowski sum volumes

We have one step left of our program towards proving Theorem 4.8. Recall that Bernshtein's Theorem uses the mixed volume $MV(\mathcal{N}(g_1), \mathcal{N}(g_2), \mathcal{N}(g_3), \mathcal{N}(g_4))$ to bound the number of isolated solutions in $\mathbf{V}(g_1, g_2, g_3, g_4) \cap (\mathbb{C} \setminus \{0\})^4$. The mixed volume, defined in Definition 1, is the coefficient of the monomial $\lambda_1 \lambda_2 \lambda_3 \lambda_4$ as it appears in the expression for the volume of the Minkowski sum $\sum_{i=1}^4 \lambda_i \mathcal{N}(g_i)$. In Lemma 4.5 we showed that this Minkowski sum can be expressed as the polytope $P_2((\mu_1 + \mu_2 + \lambda_4)m, \mu_1 l_1 + \mu_2 l_2, (\mu_1 + \lambda_4)m + \mu_2 k)$. To complete the final step of our program, we should calculate the volume of a P_2 type polytope.

From the halfspace definition in Definition 3 we see that $P_2(m', l', k')$ is the closure of the set difference $P_1(m', l') \setminus P_1(m', k')$. Thus the volume of $P_2(m', l', k')$ can be calculated as the difference in volumes of $P_1(m', l')$ and $P_1(m', k')$. In turn we can calculate the volume of P_1 as the sum of four simplices that triangulate P_1 . The volume of a simplex is straightforward to calculate by taking the determinant of a matrix whose columnvectors are the offsets from a distinguished vertex of the simplex to the other vertices. For the triangulation of P_1 it is convenient to express its facets in a more combinatorial way.

Corollary 4.6. *Labeling the vertices of P_1 by the numbers from one to eight, in the same way as in Lemma 4.2, the combinatorial facet description of P_1 is*

$$\begin{aligned} F_1 &= H_{-e_1,0} \cap P_1 = \{1, 3, 4, 5, 7, 8\} & F_m &= H_{\sum e_i, m} \cap P_1 = \{2, 3, 4, 6, 7, 8\} \\ F_2 &= H_{-e_2,0} \cap P_1 = \{1, 2, 4, 5, 6, 8\} & F_l &= H_{-e_3-e_4, l} \cap P_1 = \{1, 2, 3, 5, 6, 7\} \\ F_3 &= H_{-e_3,0} \cap P_1 = \{5, 6, 7, 8\} & F_4 &= H_{-e_4,0} \cap P_1 = \{1, 2, 3, 4\} \end{aligned}$$

Proof. The statements of Lemma 4.2 and Lemma 4.3 express the vertices as intersections of hyperplanes. Inverting the relationship and expressing the facets as the set of vertices they contain ends up with the statement above. \square

We triangulate P_1 by writing it as the union of four simplices, each of which is defined by a set of five affinely independent vertices of P_1 . As long as these simplices intersect in lower-dimensional faces we obtain a triangulation of P_1 .

Corollary 4.7. *The volume of $P_1(m, l)$ is $(m - l)^3(m + 3l)4!$.*

Proof. We shall first triangulate P_1 , calculating its volume is then a matter of summing the volumes of the triangulating simplices.

Let v be a vertex of P_1 . An *opposing facet* of v is facet of P_1 that does not contain v . Assume that we have a triangulation of every opposing facet of v . The convex hull of v and a simplex in a triangulation of an opposing facet is again a simplex. By Lemma 2.4 the simplices thus obtained triangulate P_1 . The Cohen-Hickey algorithm [2, Section 3.1] triangulates a polytope by picking a vertex and recursively triangulating its opposing facets.

From the combinatorial description of P_1 given in Corollary 4.6 it is easy to read off what the facets opposing a vertex are. In that notation the vertices of P_1 are labeled $1, \dots, 8$. We start the Cohen-Hickey algorithm by selecting as the first vertex $v_1 = 1$. Its opposing facets are F_3 and F_m , the former of which is already a simplex (it is three-dimensional on four vertices).

The next step of the recursion triangulates F_m by picking $v_2 = 2$. The facets of F_m that oppose v_2 are intersections of F_m with facets of P_1 that oppose v_2 , that is, $F_m \cap F_3 = \{6, 7, 8\}$, a simplex, and $F_m \cap F_1 = \{3, 4, 7, 8\}$. At the deepest level of the recursion we triangulate $F_m \cap F_1$ by picking $v_3 = 3$ and we find the one-dimensional simplices $F_m \cap F_1 \cap F_2 = \{4, 8\}$ and $F_m \cap F_1 \cap F_3 = \{7, 8\}$. The triangulation of $F_m \cap F_1$ is depicted in Figure 18 on the following page.

Our application of the Cohen-Hickey algorithm results in the following triangulation of P_1 : $\{\{1, 5, 6, 7, 8\}, \{1, 2, 6, 7, 8\}, \{1, 2, 3, 4, 8\}, \{1, 2, 3, 7, 8\}\}$. The volume of $P_1(m, l)$ is the sum of the volumes of the simplices in this triangulation,

$$\begin{aligned}
 \text{Vol}_4(P_1(m, l)) &= \begin{vmatrix} 0 & m-l & 0 & 0 \\ 0 & 0 & m-l & 0 \\ l & 0 & 0 & 0 \\ -l & 0 & 0 & m-l \end{vmatrix} 4! + \begin{vmatrix} m-l & m-l & 0 & 0 \\ 0 & 0 & m-l & 0 \\ 0 & -l & -l & -l \\ 0 & l & l & m \end{vmatrix} 4! \\
 &+ \begin{vmatrix} m-l & 0 & 0 & 0 \\ 0 & m-l & m-l & 0 \\ 0 & 0 & -l & -l \\ 0 & 0 & l & m \end{vmatrix} 4! + \begin{vmatrix} m-l & 0 & 0 & 0 \\ 0 & m-l & 0 & 0 \\ 0 & 0 & m-l & -l \\ 0 & 0 & 0 & m \end{vmatrix} 4! \\
 &= (m-l)^3 l 4! + (m-l)^3 l 4! + (m-l)^3 l 4! + (m-l)^3 m 4! \\
 &= (m-l)^3 (m+3l) 4!.
 \end{aligned}$$

□

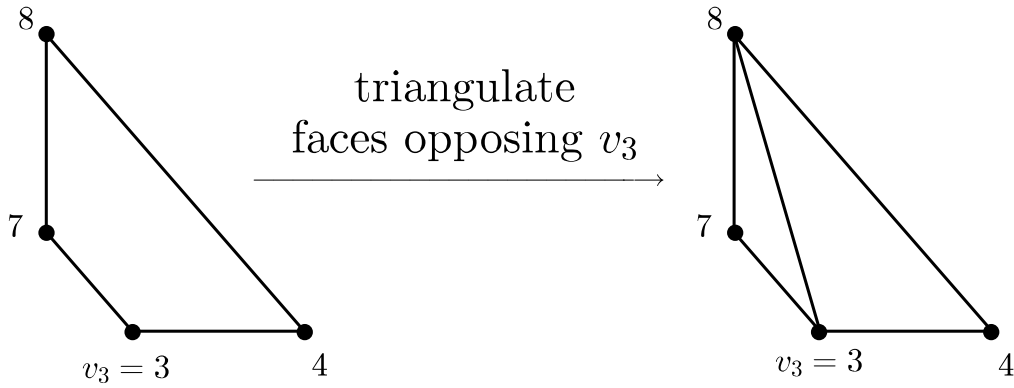


Figure 18: Triangulation of the face $F_m \cap F_3$ of P_1 , as in the proof of Corollary 4.7.

To calculate the volume of the Minkowski sum $\sum \lambda_i \mathcal{N}(g_i) = \overline{P_1(m', l') \setminus P_1(m', k')}$ we apply Corollary 4.7 and subtract the volume of $P_1(m', k')$ from that of $P_1(m', l')$. The expression for the volume we obtain is $(m' - l')^3(m' + 3l')4! - (m' - k')^3(m' + 3k')4!$.

The mixed volume of $\mathcal{N}(g_1), \mathcal{N}(g_2), \mathcal{N}(g_3), \mathcal{N}(g_4)$ can be extracted from the above volume as the coefficient of the monomial $\lambda_1 \lambda_2 \lambda_3 \lambda_4$. Extracting this coefficient by hand is somewhat tedious; Macaulay2 code that performs the necessary algebraic manipulations is included in the appendix, see Listing 1 on page 55. Recall from Section 4.4 on page 27 that for degrees two and three the polytopes P_1 and P_2 are not both four-dimensional. For these two boundary cases the code in Listing 2 on page 56 uses the PHCpack [10] interface from Macaulay2 to calculate the mixed volumes, which conform to the same formula as the $m \geq 4$ case.

At last we see that for all $m \in \mathbb{N}$ the mixed volume of the Newton polytopes $\mathcal{N}(g_1), \mathcal{N}(g_2), \mathcal{N}(g_3), \mathcal{N}(g_4)$ is $m^4 - 5m^2 + 4m$.

4.7 Applied BKK bound

We set out to prove that the number of isolated squares inscribed on an algebraic plane curve of degree m is bounded by $(m^4 - 5m^2 + 4m)/4$. In the last five sections we have shown that the variety of complex squares inscribed on a plane curve $\mathbf{V}(f)$ is defined by four polynomials g_i with the property that the mixed volume of their Newton polytopes is $(m^4 - 5m^2 + 4m)$. An immediate consequence of Bernshtein's Theorem applied to these data is that the number of isolated squares of $\mathbf{V}(g_1, g_2, g_3, g_4)$ that do not lie in a coordinate hyperplane is bounded by $(m^4 - 5m^2 + 4m)$. By passing to a different choice of coordinates we can assume no isolated squares lie in any coordinate hyperplane. Finally, as there are four parametrizations of every square inscribed on $\mathbf{V}(f)$ we divide the mixed volume by four and have proven Theorem 4.8.

Theorem 4.8. *Let $f \in \mathbb{C}[x, y]$ of degree m define an algebraic plane curve $\mathbf{V}(f) \subset \mathbb{C}^2$. The number of isolated squares inscribed on $\mathbf{V}(f)$ is at most $(m^4 - 5m^2 - 4m)/4$.*

Degree m	# solutions	squares	fraction	field
3	48	12	4991/5000	\mathbb{Q}
4	192	48	4998/5000	\mathbb{Q}
5	520	130	100/100	\mathbb{Q}
6	1140	285	50/50	$\mathbb{Z}/32479$
7	2184	546	1/1	$\mathbb{Z}/32479$
8	3808	952	1/1	$\mathbb{Z}/32479$
9	6192	1548	1/1	$\mathbb{Z}/32479$
10	9540	2385	1/1	$\mathbb{Z}/32479$

Table 4: Experimental results for number of complex squares calculated using Listing 3 on page 56. The fraction column harbors the fraction of the sample of curves that attain the maximal number of squares.

5 Experimental evidence for the number of complex squares

How many squares can be inscribed on an algebraic plane curve? Theorem 4.8 states that at most $(m^4 - 5m^2 + 4m)/4$ isolated squares are inscribed on a plane curve of degree m . Is this bound sharp, and if so, how often?

Table 4 tabulates, for degrees three to ten, the number of squares (possibly with multiplicities) inscribed on the majority of plane curves from a sample of randomly chosen curves. The experiments were carried out using the computer algebra system Macaulay2 [9], the code used is listed in Listing 3 on page 56. In all the cases the varieties turned out to be zero-dimensional, in which case all the squares inscribed on a curve are isolated. Note that the number of squares found on the curves of the sample, entered in the third column of Table 4, agrees exactly with the maximum $(m^4 - 5m^2 + 4m)/4$ provided by Theorem 4.8. Not only is the bound sharp, these experiments suggest that the bound is attained for *all* squares inscribed on a generic curve. Proving this stronger result is out of scope for the current thesis.

The curves featuring in Table 4 were generated by having Macaulay2 randomly pick the coefficients c_γ of $f = \sum_{|\gamma| \leq m} c_\gamma x^{\gamma_1} y^{\gamma_2}$ for a fixed degree m . As the degree goes up the memory usage grows. Even a degree six curve already used more than fourteen gigabytes of memory when working with the rationals as a base field. Computations for degree seven ran out of memory after using more than fifty gigabytes. For this reason finite fields were used in the calculations with higher degrees.

6 Illustrative examples of real squares

The previous section argues that there is not much of interest going on in the complex case, almost all complex algebraic plane curves inscribe the maximum number of squares. For real plane curves, however, we have no evidence as to what the generic case is.

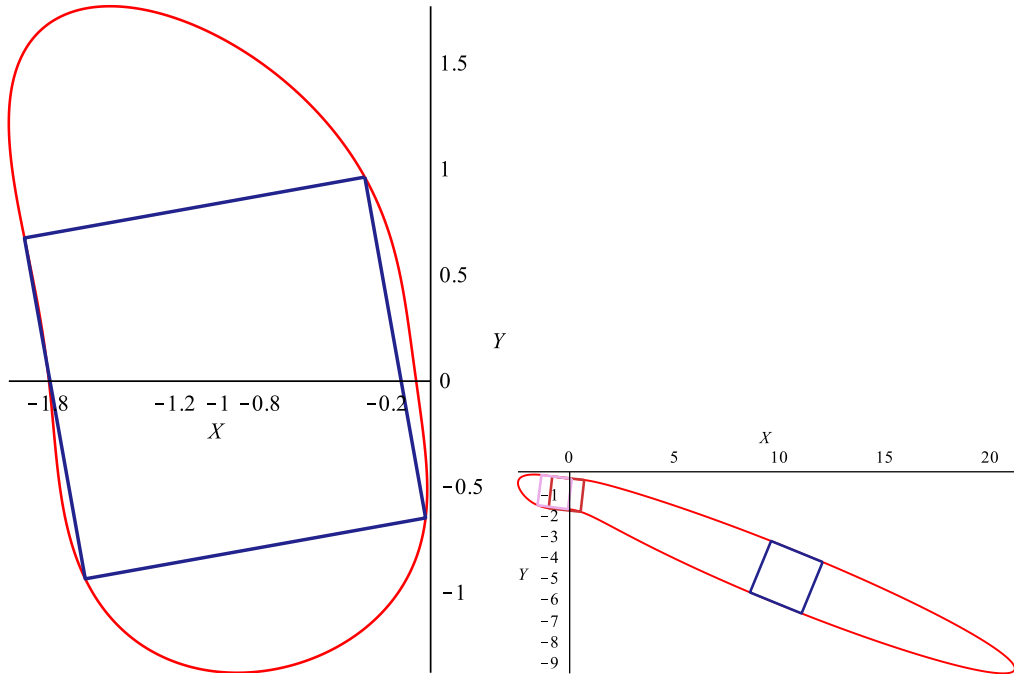
This section contains selected real plane curves of low degree that inscribe varying numbers of squares. The pictures have been plotted in Maple, using the code from Listing 6 on page 60, based on numerical data for the locations of the squares computed by PHCPack [10]. The topology of the curves has been determined by a manual process: the RAGlib [21] Maple package provides at least one point on each connected component of a plane curve, by inspecting the plot and intersecting the curves with suitably chosen lines we can determine which visible components connect outside of the plotted range. The “realroots.m2” functionality written by Dan Grayson and Frank Sottile [24] was used for determining how many real intersections these lines and the curves have. The polynomials that define the curves in the plots are listed in Table 7 on page 52.

The maximal number of squares inscribed on a third degree curve is twelve, according to Theorem 4.8; the examples in this section show that a third degree real curve can inscribe any number of squares from zero to twelve, see Table 6a on page 39. Two topological types attaining the maximum number are shown in Figure 22 on page 42 and Figure 28 on page 48. Curves of these types look like perturbations of either a) an oval times a line, or b) the product of three lines. The perturbation approach of constructing curves is called the “marking method” by Gudkov [11, Section 2.10].

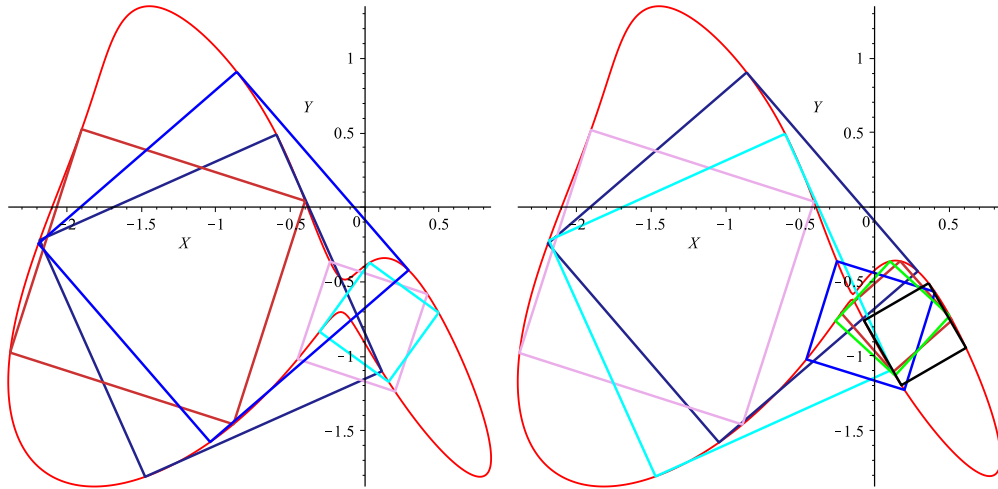
The proofs of Emch, Jerrard and Stromquist establish that, generically, on a smooth enough Jordan curve the number of inscribed squares will be odd. It is no surprise then that we see the same behaviour for algebraic plane curves that topologically speaking are circles. Figure 19 on the next page shows algebraic Jordan curves inscribing one, three, five and seven squares.

Recall that a Jordan curve starts and ends at the same point without intersecting itself, it is closed and simple. A Jordan curve has only one connected component and it is homeomorphic to a circle. Unlike Jordan curves, a simple algebraic plane curve can consist of multiple components, and the components can be homeomorphic to a circle or to the real line. Table 5 on page 39 tabulates the number of squares found on plane curves computed for this thesis with the code from Listing 4 on page 57; the rows of the table are indexed by the number of components homeomorphic to the real line, and the columns are indexed by the number of components homeomorphic to a circle (called ovals).

The example curves homeomorphic to a real line, as well as some other topological types of curves, exhibit a parity condition on the number of inscribed squares just as in the Jordan case, see Section 6.1 on page 39. The types for which this occurs have their entries shaded gray in Table 5 on page 39. Whether this parity condition is an actual property of these curves or an artifact of our selection of examples remains to be seen. Other topological types have both an odd and an even number of squares, these are listed in Section 6.2 on page 44.



(19.a) One square inscribed on f_{30} in Table 7 on page 52 (19.b) Three squares inscribed on f_{31} in Table 7 on page 52



(19.c) Five squares inscribed on f_{32} in Table 7 on page 52 (19.d) Seven squares inscribed on f_{33} in Table 7 on page 52

Figure 19: Algebraic Jordan curves inscribing an odd number of squares.

lines i \ ovals j	0	1	2	3	4
0		1, 3, 5, 7	0, 2, 4, 6, 16		8
1	0, 2, 4, 6, 12	1, 2*, 3, 5, 7, 9, 11			
2	1, 4, 8, 9, 11	3, 5, 7			
3	1, 4, 7, 8, 10, 11, 12	8, 9, 11			

Table 5: Number of squares inscribed on curves of degree up to five. The (i, j) -th cell corresponds to curves homeomorphic to i copies of the real line and j copies of the circle. The entry 2* in the $(1, 1)$ cell corresponds to Figure 25.b on page 45.

The 2 that occurs in the entry for curves that consist of one line and one oval corresponds to Figure 25.b on page 45. Inclusion of this reducible curve is debatable. If one allows reducible curves, then taking unions of lower degree curves will construct examples where the total number of inscribed squares is the sum of the squares inscribed on each curve in the union, each part behaving independently. At this point it is not clear to us whether reducible curves should be excluded.

	0	1		0	1	2	3	4
0			0		1, 3, 5, 7	0, 2, 4, 6, 16		8
1	0, 2, 6, 12	1, 2, 3, 5, 7, 9, 11	1					
2			2	4, 8, 9, 11	3, 5, 7			
3	4, 7, 8, 10, 11, 12		3					

(a) Squares inscribed on degree three curves (b) Squares inscribed on degree four curves

Table 6: Number of squares inscribed on curves of degree three and four. The (i, j) -th cell corresponds to curves homeomorphic to i copies of the real line and j copies of the circle.

6.1 Topological types of curves with a possible parity condition on the number of inscribed squares

6.1.1 One topological line inscribing an even number of squares

A straight line does not inscribe any squares. Among the curves computed for this thesis, all of the curves that consist of one topological component homeomorphic to the real line inscribe an even number of squares. Included are two examples of cubic curves inscribing the maximal number of twelve squares: Figure 22 on page 42 and Figure 21.f on page 41. The other curves in Figure 21 on page 41 inscribe zero, two, four and six squares.

Curves that are homeomorphic to a real line but not necessarily algebraic are not restricted by this parity condition of inscribing an even number of squares. Consider the curve, displayed in Figure 20 on the following page, consisting of two parallel rays in opposite directions, connected by a line segment at a fortyfive degree angle to both the rays. This curve inscribes one square, it has the line segment BC as a diagonal.

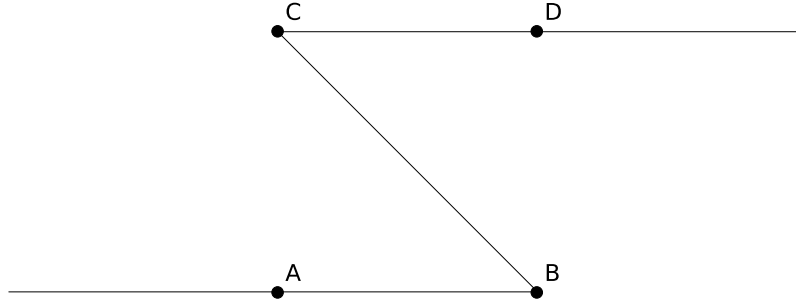


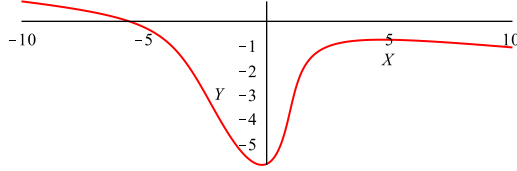
Figure 20: A topological line inscribing one square.

6.1.2 Pairs of ovals inscribing an even number of squares

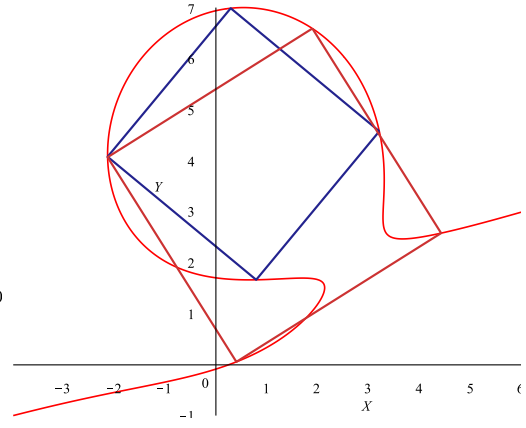
The curves in Figure 23 on page 43 consist of two ovals and inscribe zero, two, four, six and sixteen isolated squares. The curves in Figure 23.a on page 43 and Figure 23.e on page 43 are of the form $(X^2 + Y^2/4 - 1)(X^2/4 + Y^2 - 1) + k$. If (X, Y) lies on such a curve, then by symmetry it forms one corner of a square centered at the origin. The squares depicted in Figures 23.a and 23.e are the squares that do not lie on the positive-dimensional components of respectively $\mathbf{V}(I_{f_{41}})$ and $\mathbf{V}(I_{f_{45}})$.

6.1.3 An oval and two lines inscribing an odd number of squares

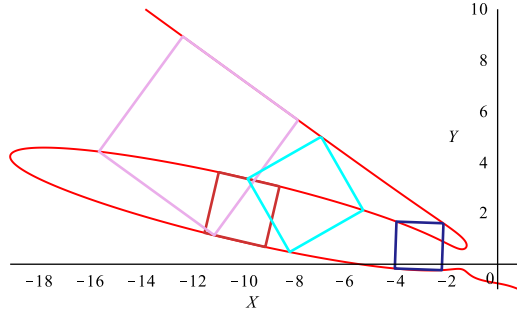
The curves in Figure 24 on page 44 inscribe an odd number of squares: three, five and seven.



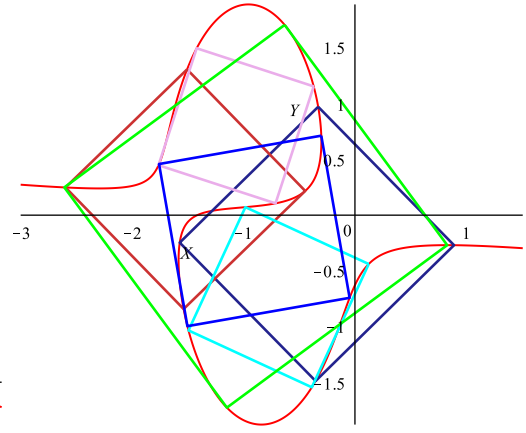
(21.a) Zero squares inscribed on f_1 in Table 7 on page 52



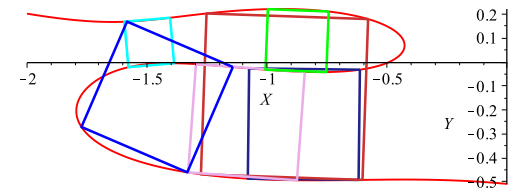
(21.b) Two squares inscribed on f_2 in Table 7 on page 52



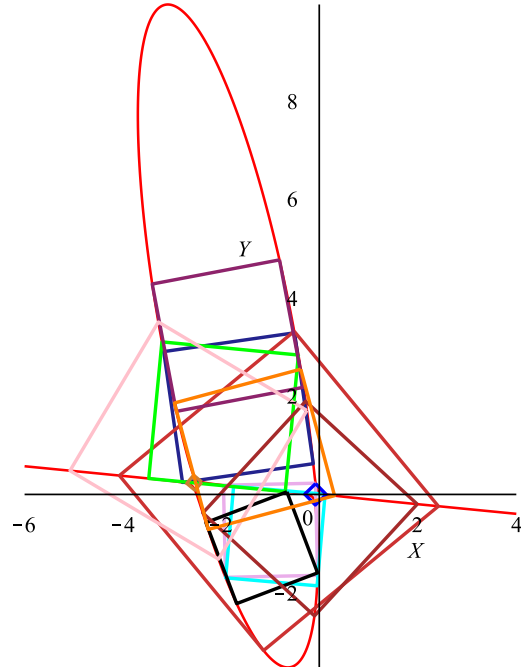
(21.c) Four squares inscribed on f_3 in Table 7 on page 52



(21.d) Six squares inscribed on f_4 in Table 7 on page 52



(21.e) Six squares inscribed on f_5 in Table 7 on page 52



(21.f) Twelve squares inscribed on f_6 in Table 7 on page 52

Figure 21: An even number of squares inscribed on a line.

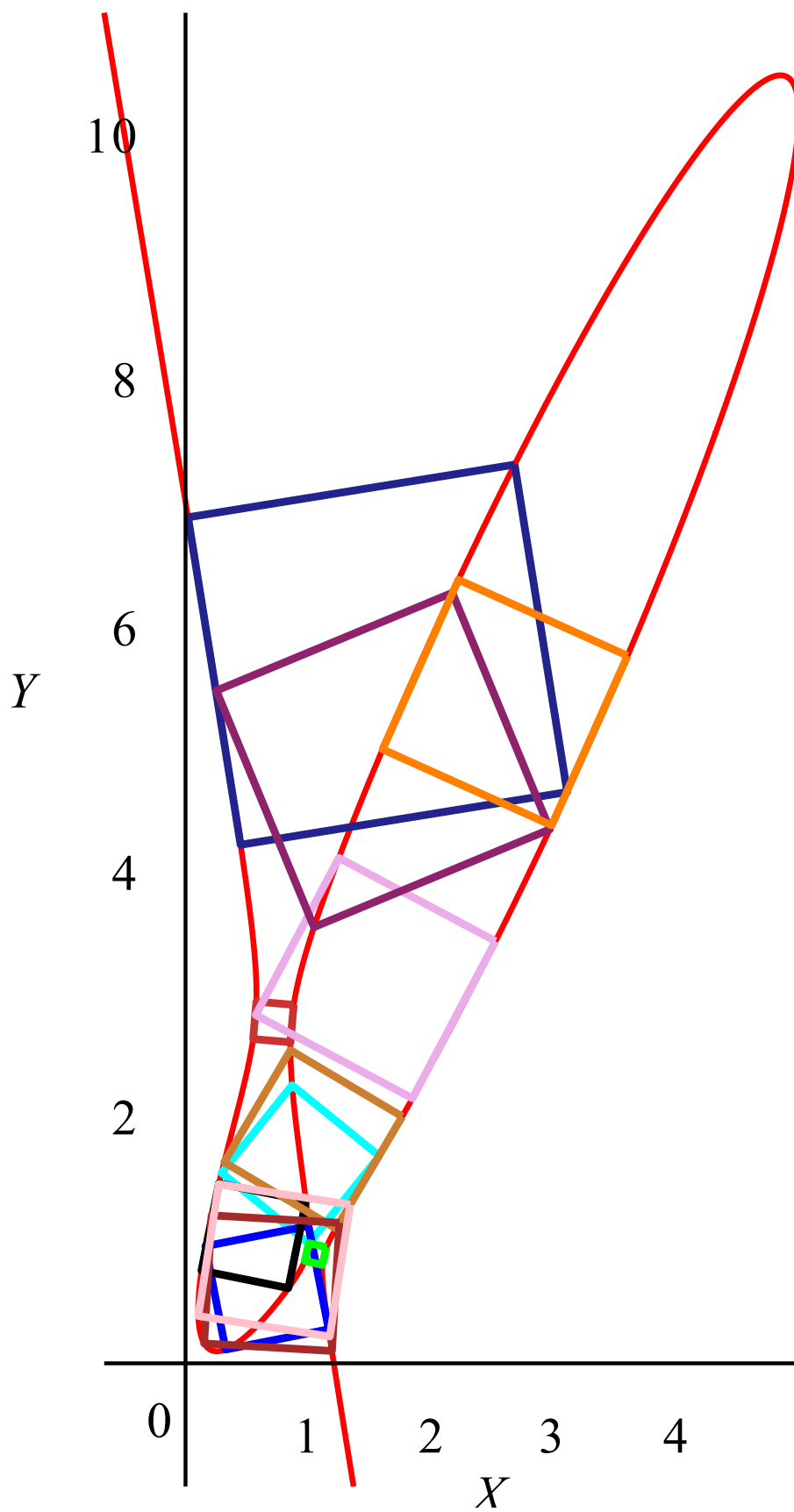
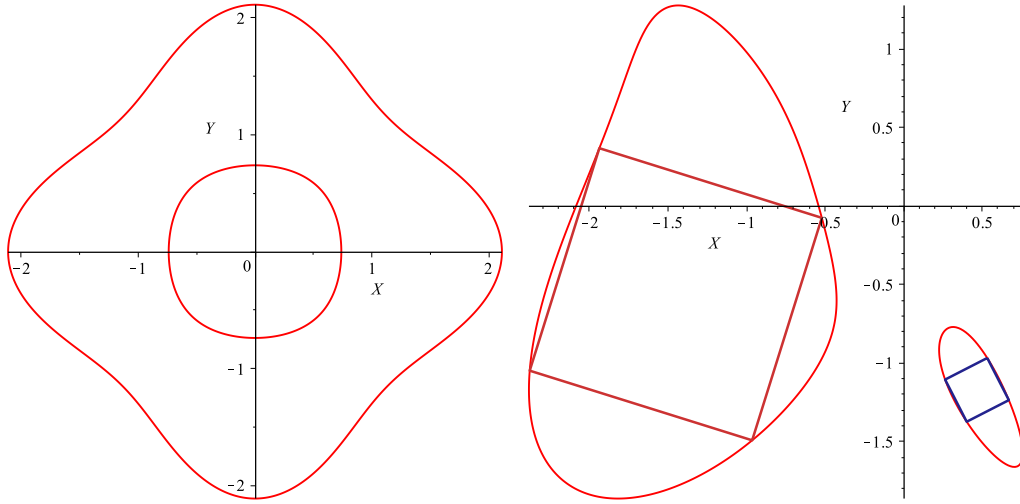
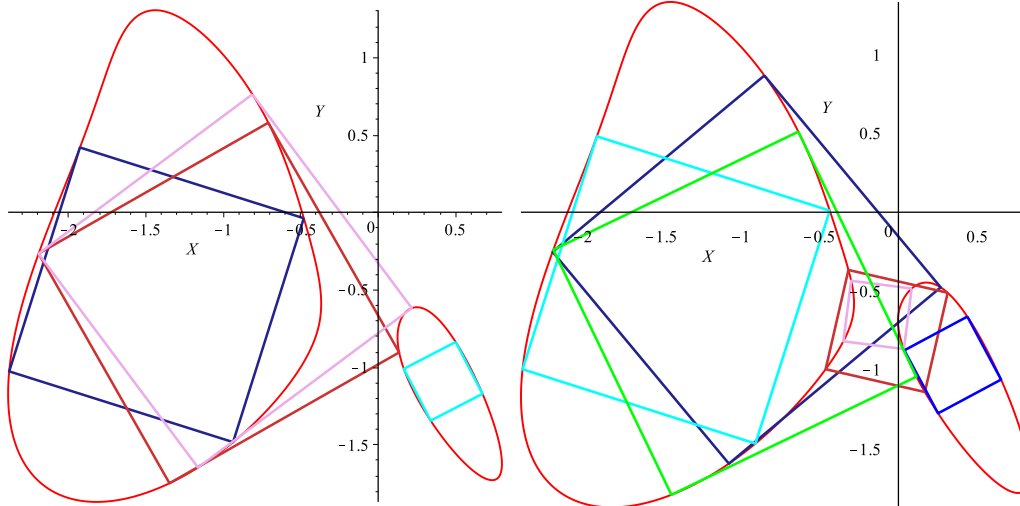


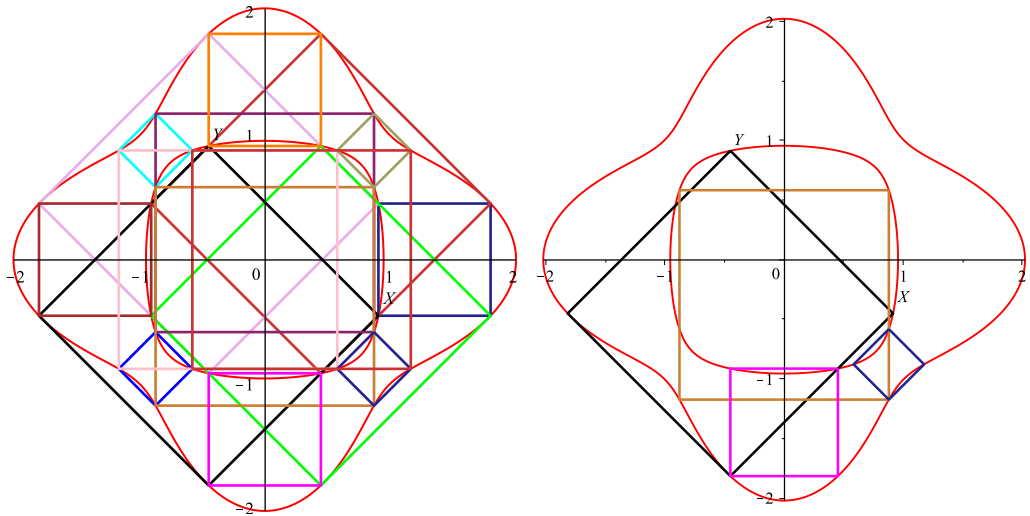
Figure 22: Twelve squares inscribed on f_7 in Table 7 on page 52



(23.a) Zero squares inscribed on f_{41} in Table 7 on page 52 (23.b) Two squares inscribed on f_{42} in Table 7 on page 52

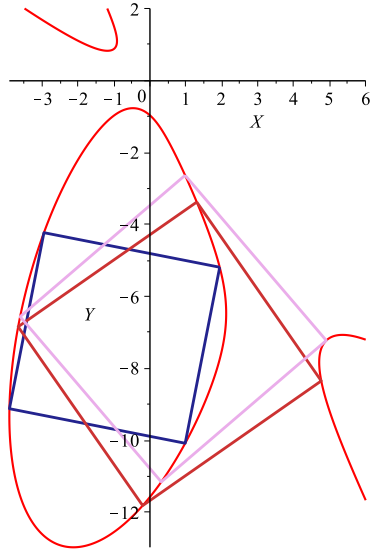


(23.c) Four squares inscribed on f_{43} in Table 7 on page 52 (23.d) Six squares inscribed on f_{44} in Table 7 on page 52

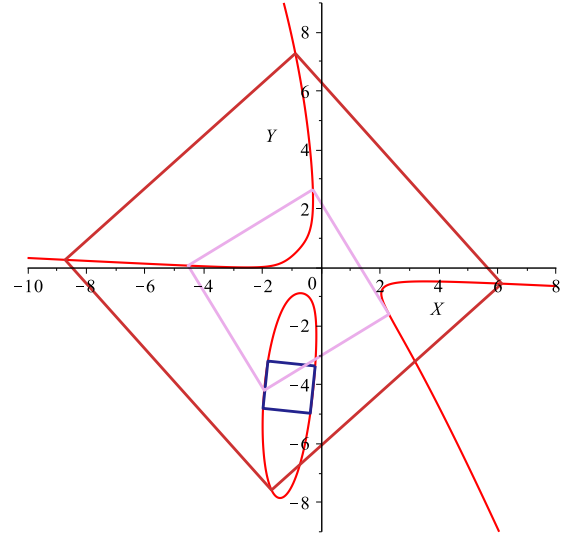


(23.e) Sixteen squares inscribed on f_{45} in Table 7 on page 52 (23.f) Up to rotational symmetry, four squares inscribed on f_{45}

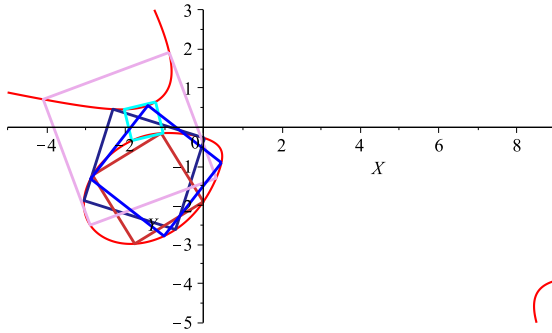
Figure 23: Two ovals inscribing an even number of squares.



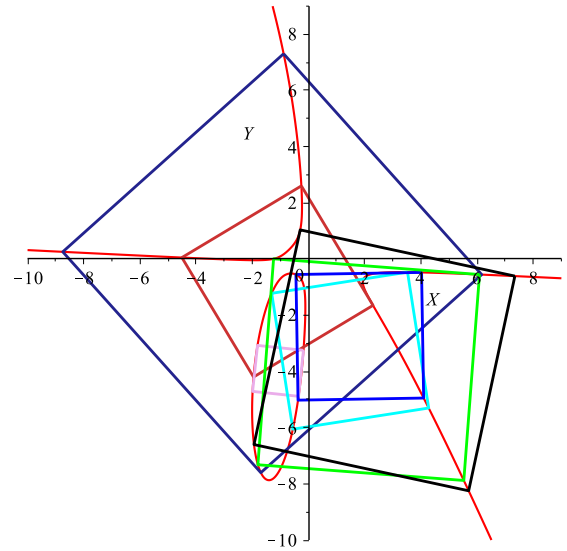
(24.a) Three squares inscribed on f_{34} in Table 7 on page 52



(24.b) Three squares inscribed on f_{35} in Table 7 on page 52



(24.c) Five squares inscribed on f_{36} in Table 7 on page 52



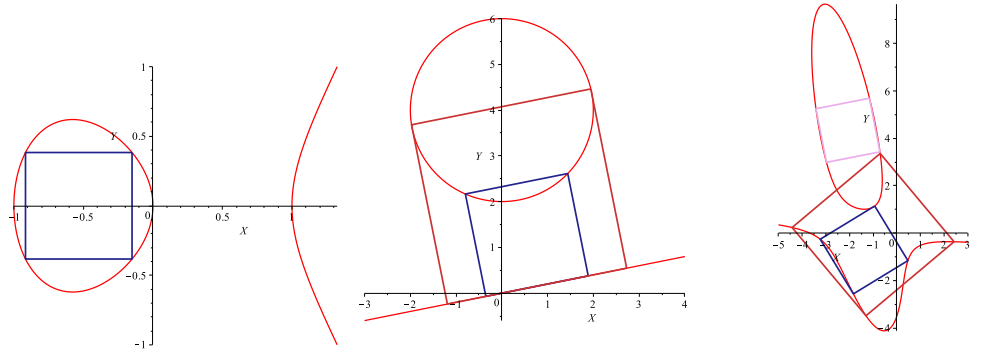
(24.d) Seven squares inscribed on f_{37} in Table 7 on page 52

Figure 24: An oval and two lines inscribing an odd number of squares.

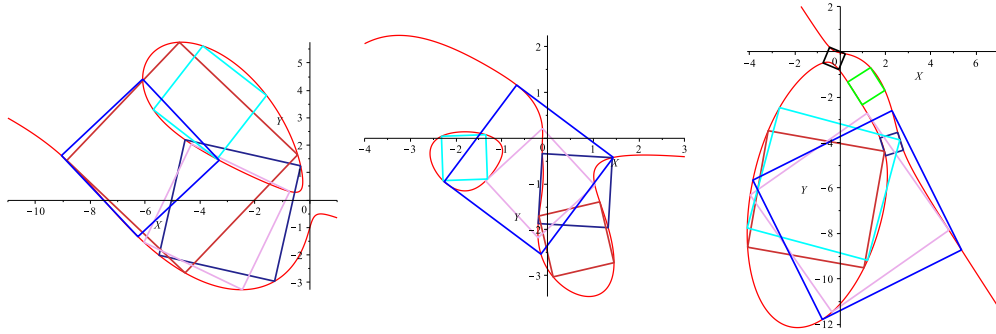
6.2 Topological types of curves lacking a parity condition on the number of inscribed squares

6.2.1 Squares inscribed on one oval and one line

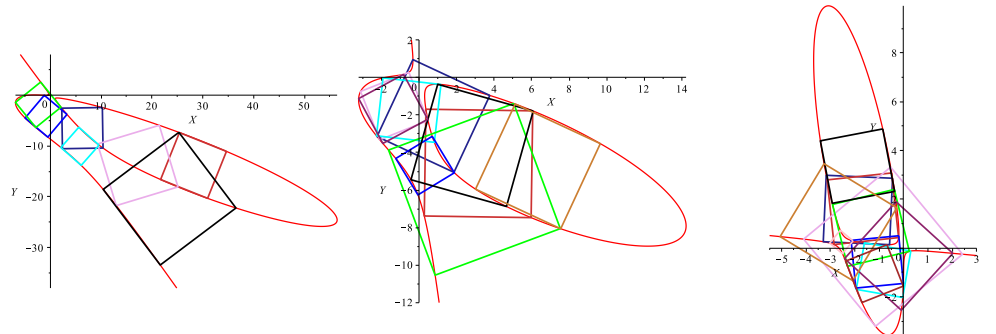
The curves in Figure 25 on the next page inscribe one, two, three, five, seven, nine and eleven squares. Note that the curve in Figure 25.b is reducible.



(25.a) One square inscribed on f_{18} in Table 7 on page 52
 (25.b) Two squares inscribed on f_{19} in Table 7 on page 52
 (25.c) Three squares inscribed on f_{20} in Table 7 on page 52



(25.d) Five squares inscribed on f_{21} in Table 7 on page 52
 (25.e) Five squares inscribed on f_{22} in Table 7 on page 52
 (25.f) Seven squares inscribed on f_{23} in Table 7 on page 52

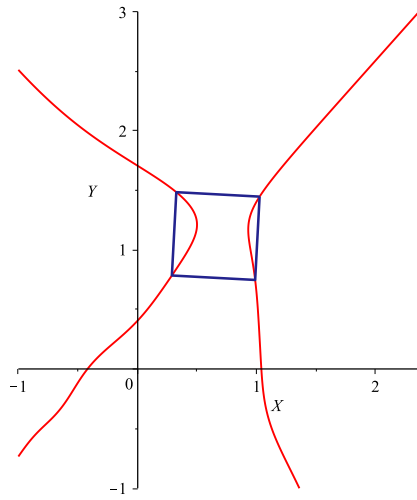


(25.g) Seven squares inscribed on f_{24} in Table 7 on page 52
 (25.h) Nine squares inscribed on f_{25} in Table 7 on page 52
 (25.i) Eleven squares inscribed on f_{26} in Table 7 on page 52

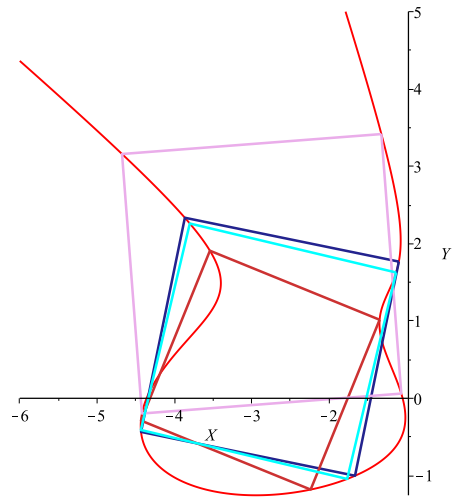
Figure 25: Squares inscribed on an oval and a line.

6.2.2 Squares inscribed on two lines

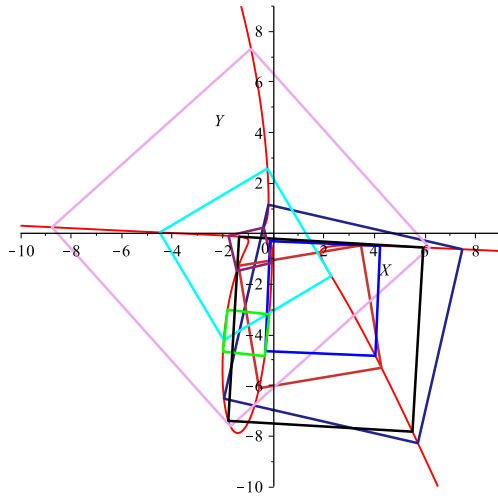
The curves in Figure 26 on the following page inscribe one, four, eight, nine and eleven squares.



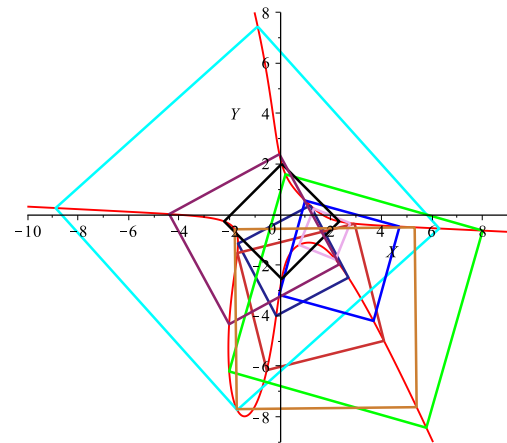
(26.a) One square inscribed on f_{13} in Table 7 on page 52



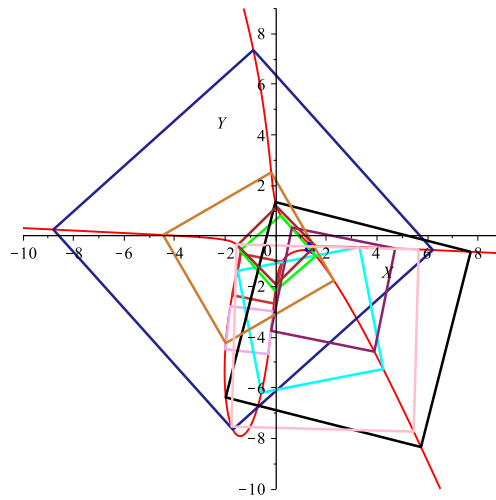
(26.b) Four squares inscribed on f_{14} in Table 7 on page 52



(26.c) Eight squares inscribed on f_{15} in Table 7 on page 52



(26.d) Nine squares inscribed on f_{16} in Table 7 on page 52

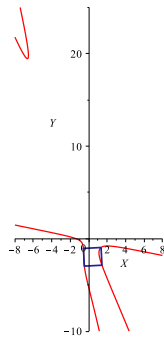


(26.e) Eleven squares inscribed on f_{17} in Table 7 on page 52

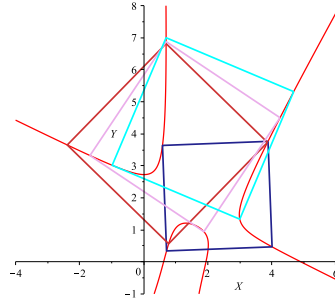
Figure 26: Squares inscribed on two lines.

6.2.3 Squares inscribed on three lines

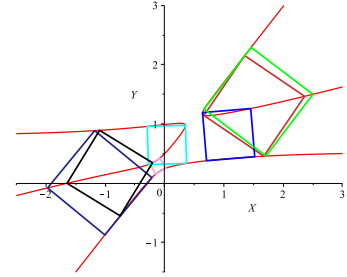
The curves in Figure 27 inscribe one, four, seven, eight, ten and eleven squares. Figure 28 on the following page depicts a third degree curve consisting of three lines inscribing the maximal number of twelve squares.



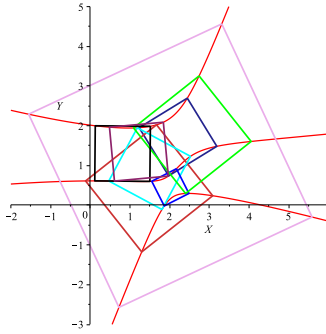
(27.a) One square inscribed on f_8 in Table 7 on page 52



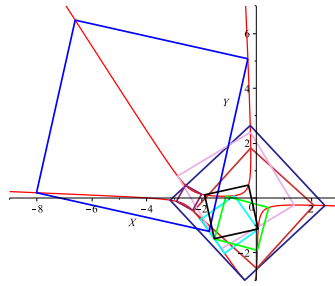
(27.b) Four squares inscribed on f_9 in Table 7 on page 52



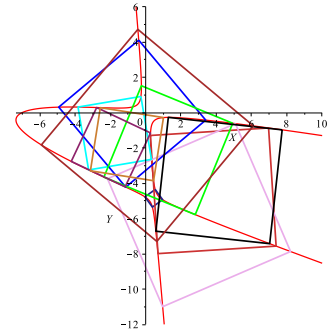
(27.c) Seven squares inscribed on f_{10} in Table 7 on page 52



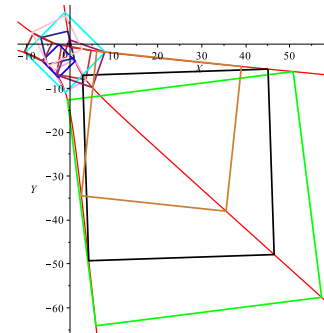
(27.d) Eight squares inscribed on f_{11} in Table 7 on page 52



(27.e) Eight squares inscribed on f_{38} in Table 7 on page 52



(27.f) Ten squares inscribed on f_{39} in Table 7 on page 52



(27.g) Eleven squares inscribed on f_{40} in Table 7 on page 52

Figure 27: Squares inscribed on three lines.

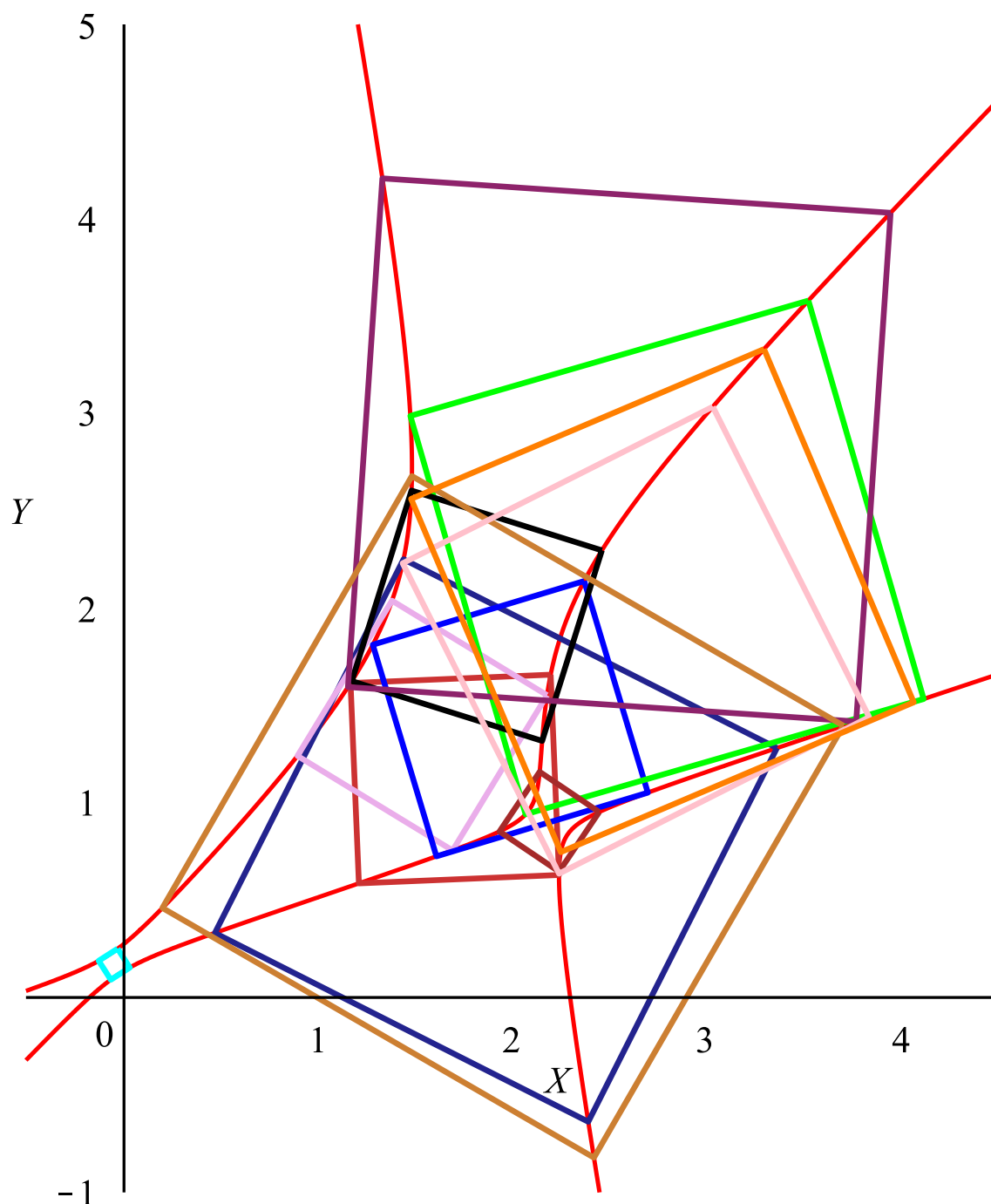
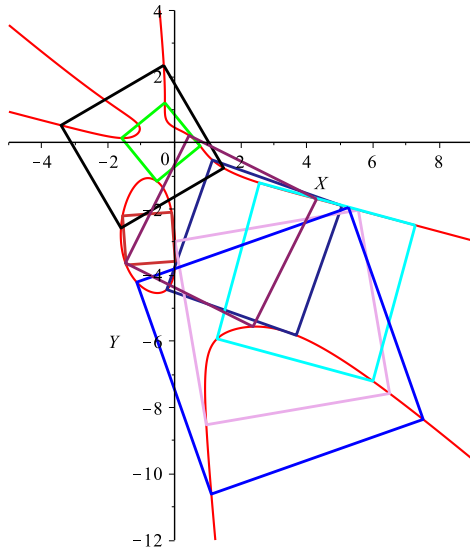


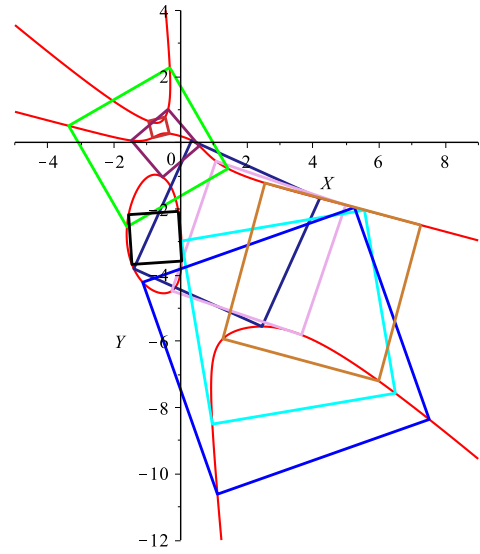
Figure 28: Twelve squares inscribed on f_{12} in Table 7 on page 52

6.2.4 Squares inscribed on an oval and three lines

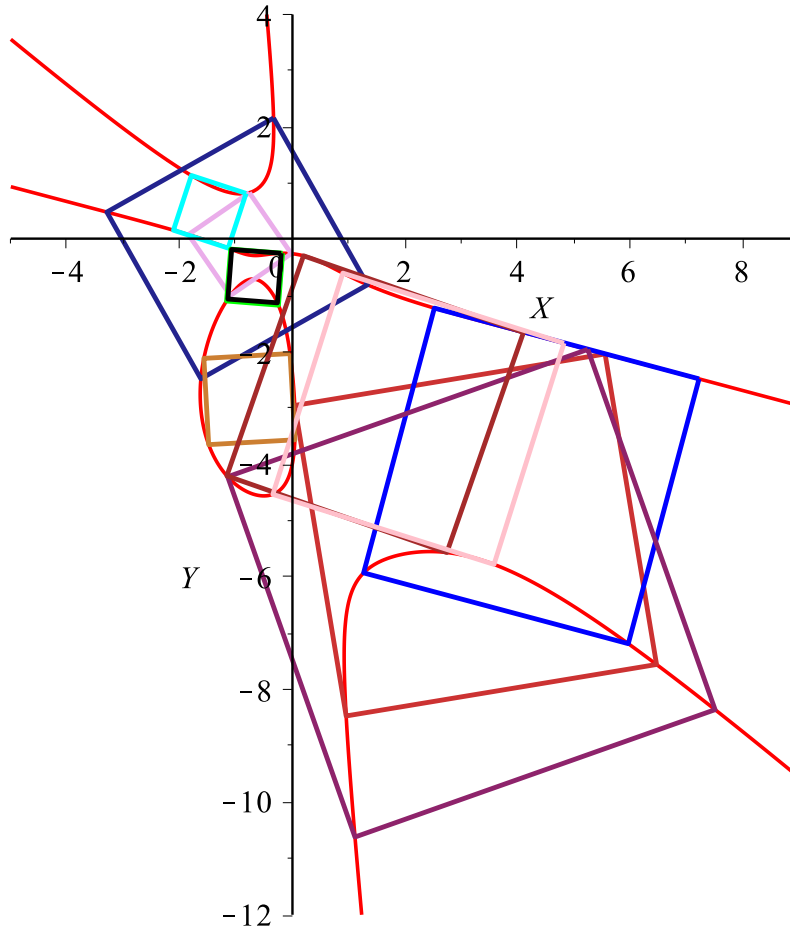
The curves in Figure 29 on the next page inscribe eight, nine and eleven squares.



(29.a) Eight squares inscribed on f_{27} in Table 7 on page 52



(29.b) Nine squares inscribed on f_{28} in Table 7 on page 52



(29.c) Eleven squares inscribed on f_{29} in Table 7 on page 52

Figure 29: Squares inscribed on an oval and three lines.

7 Concluding remarks

The main result of this thesis, Theorem 4.8 in Section 4 on page 21, shows that the number of isolated squares inscribed on a degree m complex algebraic plane curve is at most $(m^4 - 5m^2 + 4m)/4$. The experimental evidence of Section 5 on page 36 suggests this statement might be strengthened to “a generic complex algebraic plane curve inscribes precisely $(m^4 - 5m^2 + 4m)/4$ squares”. Whether that is true or not, one can ask for any natural number m what the maximum attainable number of isolated inscribed squares is on a curve of degree m . Can we construct a curve that attains the theoretical maximum of $(m^4 - 5m^2 + 4m)/4$? At least up to degree five any of the curves of Table 4 on page 36 provides a positive answer, but we should aim for a theoretical argument for all degrees. Following Rojas [20, Section 3.3, p7], giving the conditions when the maximum number of solutions is attained might be fruitful. Intersection theory may also apply to show that the complex squares from Table 4 on page 36 have multiplicity one.

Restricting these questions to real plane curves we can ask again, is there a real algebraic plane curve that attains the bound of Theorem 4.8? Section 6 on page 36 includes several positive examples for degree three.

Certain symmetries in a plane curve give rise to an infinite number of inscribed squares. The author is however not aware of a complete classification of which kinds of curves inscribe an infinitude of squares.

Based on the shaded cells of Table 5 on page 39 we could conjecture: Is it true that algebraic plane curves homeomorphic to one of

1. the real line
2. an oval and two lines
3. two ovals

inscribe respectively an even, odd, and even number of squares? The other shaded cell corresponds to algebraic Jordan curves, for which it is already known that this class of curves generically inscribes an odd number of squares.

Approximating a general Jordan curve with a subclass of curves for which we know Toeplitz’s conjecture to be true may fail to produce an inscribed square in the limit if the approximating squares degenerate to a point. Pak [18, Section 3.7] remarks that nonetheless the limit argument has its use; for an approximation argument by algebraic curves we will need to have control over the sizes of the squares to prevent the squares from degenerating in the limit.

References

- [1] D. Bernshtein. The number of roots of a system of equations. *Funct. Anal. Appl.*, 9(3):183–185, 1975.

- [2] B. Büeler, A. Enge and K. Fukuda. Exact volume computation for polytopes: A practical study. In G. Kalai and G. Ziegler, editors, *Polytopes — Combinatorics and Computation*, volume 29 of *DMV Seminar*, pages 131–154. Birkhäuser Basel, 2000.
- [3] D. Cox, J. Little and D. O’Shea. *Using algebraic geometry*, volume 185 of *Graduate Texts in Mathematics*. Springer-Verlag, New York, 1998.
- [4] D. Cox, J. Little and D. O’Shea. *Ideals, varieties, and algorithms: An introduction to computational algebraic geometry and commutative algebra*. Undergraduate Texts in Mathematics. Springer, New York, third edition, 2007.
- [5] H. G. Eggleston. Figures inscribed in convex sets. *Amer. Math. Monthly*, 65(2):76–80, 1958.
- [6] D. Eisenbud. *Commutative algebra: With a view toward algebraic geometry*, volume 150 of *Graduate Texts in Mathematics*. Springer-Verlag, New York, 1995.
- [7] A. Emch. Some properties of closed convex curves in a plane. *Amer. J. Math.*, 35(4):407–412, 1913.
- [8] A. Emch. On some properties of the medians of closed continuous curves formed by analytic arcs. *Amer. J. Math.*, 38(1):6–18, 1916.
- [9] D. R. Grayson and M. E. Stillman. Macaulay2 version 1.6, a software system for research in algebraic geometry. Available at <http://www.math.uiuc.edu/Macaulay2/>.
- [10] E. Gross, S. Petrović and J. Verschelde. Interfacing with PHCpack. *J. Softw. Algebra Geom.*, 5:20–25, 2013.
- [11] D. A. Gudkov. The topology of real projective algebraic varieties. *Russian Math. Surveys*, 29(4):1–79, Aug. 1974.
- [12] B. Huber and B. Sturmfels. Bernstein’s theorem in affine space. *Discrete Comput. Geom.*, 17(2):137–141, 1997.
- [13] R. P. Jerrard. Inscribed squares in plane curves. *Trans. Amer. Math. Soc.*, 98:234–241, 1961.
- [14] B. Matschke. A survey on the Square Peg Problem. *Notices Amer. Math. Soc.*, 61(4):346–352, 2014.
- [15] M. D. Meyerson. Balancing acts. In *The Proceedings of the 1981 Topology Conference (Blacksburg, Va., 1981)*, volume 6, pages 59–75 (1982), 1981.
- [16] M. J. Nielsen. Triangles inscribed in simple closed curves. *Geom. Dedicata*, 43(3):291–297, 1992.

- [17] I. Pak. Lectures on Discrete and Polyhedral Geometry. Book in progress, accessed March 2014. Available at <http://www.math.ucla.edu/~pak/book.htm>.
- [18] I. Pak. The discrete square peg problem, 2008, arXiv:0804.0657. preprint, 10pp.
- [19] S. G. Popvassilev. On the number of inscribed squares of a simple closed curve in the plane, 2008, arXiv:0810.4806. preprint, 5pp.
- [20] J. M. Rojas. Toric intersection theory for affine root counting. *J. Pure Appl. Algebra*, 136(1):67–100, 1999.
- [21] M. Safey El Din. RAGLib version 3.21, a Maple package for real solving polynomial systems of equations and inequalities. Available at <http://www-polysys.lip6.fr/~safey/RAGLib/>.
- [22] F. Sagols and R. Marín. The inscribed square conjecture in the digital plane. In *Combinatorial image analysis*, volume 5852 of *Lecture Notes in Comput. Sci.*, pages 411–424. Springer, Berlin, 2009.
- [23] R. Schneider. *Convex bodies: the Brunn-Minkowski theory*, volume 44 of *Encyclopedia of Mathematics and its Applications*. Cambridge University Press, Cambridge, 1993.
- [24] F. Sottile. From enumerative geometry to solving systems of polynomials equations. In *Computations in algebraic geometry with Macaulay 2*, volume 8 of *Algorithms Comput. Math.*, pages 101–129. Springer, Berlin, 2002.
- [25] P. Stein. Classroom Notes: A note on the volume of a simplex. *Amer. Math. Monthly*, 73(3):299–301, 1966.
- [26] W. Stromquist. Inscribed squares and square-like quadrilaterals in closed curves. *Mathematika*, 36(2):187–197 (1990), 1989.
- [27] G. M. Ziegler. *Lectures on polytopes*, volume 152 of *Graduate Texts in Mathematics*. Springer-Verlag, New York, 1995.

Appendix

Table of polynomials

Table 7: Polynomials defining curves in Section 6 on page 36.

$$f_1 \quad (3/8)x^3 + 4x^2y + (10/7)xy^2 + (2/7)y^3 + x^2 + 10xy + (7/9)y^2 + (1/7)x + (4/5)y + 10369/300$$

Table 7: Polynomials defining curves

$$\begin{aligned}
f_2 & -(1013346057932523458320374654611/2350924922880000000000)x^3+ \\
& (2584640714944881315625401696659/1959104102400000000000)x^2y- \\
& (24370961833016176942717940959039/58773123072000000000000)xy^2+ \\
& (495964933561657788423357606871/4897760256000000000000)y^3- \\
& (17651791649159643199956179410837/23509249228800000000000)x^2+ \\
& (255915596711949314264306252576989/117546246144000000000000)xy- \\
& (5664920610070897911630510019033/6530347008000000000000)y^2- \\
& (45022793169990743253008147707121/117546246144000000000000)x+ \\
& (659705135608555410904182133087481/587731230720000000000000)y+ \\
& 12665836021084318920971168631593/117546246144000000000000 \\
f_3 & (1/7)x^5+(6/7)x^4y+(9/5)x^3y^2+x^2y^3+7xy^4+10y^5+x^4+(4/5)x^3y+(10/7)x^2y^2+3xy^3+(7/5)y^4+ \\
& (7/6)x^3+(1/8)x^2y+(3/4)xy^2+(1/3)y^3+(3/10)x^2+(4/5)xy+(5/3)y^2+(5/3)x+(10/9)y+9/4 \\
f_4 & (1/2)x^3+5x^2y+(2/9)xy^2+(5/6)y^3+(9/7)x^2+9xy+(1/9)y^2+(7/5)x+(10/9)y+5/6 \\
f_5 & (1/3)x^3+x^2y+(7/9)xy^2+9y^3+(10/9)x^2+2xy+(7/2)y^2+(8/7)x+(1/10)y+1/3 \\
f_6 & (3/8)x^3+4x^2y+(10/7)xy^2+(2/7)y^3+x^2+10xy+(7/9)y^2+(1/7)x+(4/5)y-19/600 \\
f_7 & (32357486150754911/3402639576000000)x^3-(14565996465296101997/2143662932880000000)x^2y+ \\
& (93487619285326211413/135050764771440000000)xy^2+(295881163208333/837368333156250)y^3- \\
& (16455993365369237399/1071831466440000000)x^2 \\
& +(2262751792681121895697/270101529542880000000)xy \\
& -(44377450778015156987/16881345596430000000)y^2 \\
& +(483511249013004548209/900338431809600000000)x \\
& +(43079601667153982323/337626911928600000000)y-9025382297117723393/11254230397620000000 \\
f_8 & (4/3)x^5+7x^4y+(7/3)x^3y^2+(1/2)x^2y^3+(1/2)xy^4+(1/10)y^5+(10/7)x^4+(7/3)x^3y+(2/5)x^2y^2+ \\
& (2/3)xy^3+(5/9)y^4+(3/2)x^3+3x^2y+xy^2+(1/3)y^3+4x^2+(2/3)xy+(8/9)y^2+(8/3)x+(1/10)y+7/5 \\
f_9 & (84600046159243700856114369758453/7304069487211315200000000)x^3+ \\
& (84129864593783714477250895601927/4869379658140876800000000)x^2y- \\
& (92678186386758381841697632332217/7304069487211315200000000)xy^2- \\
& (985032890300878882041984922489/29216277948845260800000000)y^3- \\
& (8432107925141586913574285861810083/973875931628175360000000000)x^2- \\
& (42810357305315843166329246331701/18034739474595840000000000)xy+ \\
& (798870306331587087351224027449571/584325558976905216000000000)y^2+ \\
& (841046078607802229000433529244096647/5258930030792146944000000000)x- \\
& (50130881628172999018538048620781701/5258930030792146944000000000)y- \\
& 120544249950526645232049562396939597/1752976676930715648000000000
\end{aligned}$$

Table 7: Polynomials defining curves

f_{10}	$(17071630870821024280289/127253121732748247040000000)x^3 +$ $(44219727353738152825699/5302213405531176960000000)x^2y -$ $(4775926187801988597243641/127253121732748247040000000)xy^2 +$ $(2615354993498783429179/108208436847575040000000)y^3 -$ $(218792069736804757977449/3895503726512701440000000)x^2 +$ $(303432548905886033642387/6362656086637412352000000)xy -$ $(15987089135911642991445653/381759365198244741120000000)y^2 -$ $(86769535959101859196900919/763518730396489482240000000)x +$ $(1265378561015612782058837/610814984317191585792000000)y -$ $2225833681103904456175739/763518730396489482240000000$	
f_{11}	$-(107666602244268965505153/343597383680000000000000)x^3 +$ $(244020905347080929848137/137438953472000000000000)x^2y +$ $(3029447197152010641168729/343597383680000000000000)xy^2 -$ $(2494391888436262290669501/687194767360000000000000)y^3 -$ $(6731424554769315405645039/13743895347200000000000000)x^2 -$ $(1119679636867415864847621/429496729600000000000000)xy -$ $(88162122657769201785657501/13743895347200000000000000)y^2 +$ $(1720365306508271453007846519/137438953472000000000000000)x +$ $(5145387047581092010866673443/137438953472000000000000000)y -$ $676235828568952472903449101/343597383680000000000000000$	
f_{12}	$-(4963493942513921243/655483207680000000)x^3 + (326139891975237682121/1123685498880000000)x^2y -$ $(50931413248303191071/2996494663680000000)xy^2 - (14263797412722377/3397386240000000)y^3 +$ $(37805850432694119373/3277416038400000000)x^2 -$ $(19179033623835553860379/31463193968640000000)xy +$ $(1018795941059176616167/1997663109120000000)y^2 +$ $(1330205416456247598397/104877313228800000000)x -$ $(2843296777056554250263/139836417638400000000)y + 95073566433481051/52022476800000000$	
f_{13}	$12415x^8 + 11377x^7y + 15240x^6y^2 - 451x^5y^3 + 4672x^4y^4 + 4256x^3y^5 + 2937x^2y^6 - 14392xy^7 - 11440y^8 -$ $1118x^7 + 8649x^6y + 9988x^5y^2 + 15342x^4y^3 - 13207x^3y^4 + 4533x^2y^5 + 13680xy^6 + 9917y^7 - 8343x^6 -$ $6757x^5y - 8308x^4y^2 + 7606x^3y^3 + 3138x^2y^4 - 5358xy^5 + 11848y^6 + 12694x^5 + 181x^4y + 3136x^3y^2 -$ $12922x^2y^3 - 14700xy^4 + 9107y^5 + 9973x^4 + 1173x^3y - 15433x^2y^2 + 2406xy^3 - 13196y^4 - 8485x^3 - 8414x^2y -$ $15263xy^2 + 15206y^3 - 7714x^2 - 7243xy + 4230y^2 - 10183x + 5303y - 3662$	
f_{14}	$(10/9)x^4 + (2/7)x^3y + 2x^2y^2 + 5xy^3 + (10/7)y^4 + 5x^3 + (10/3)x^2y + (2/5)xy^2 + (1/7)y^3 + (1/2)x^2 + (10/9)xy +$ $(3/2)y^2 + (1/7)x + (5/9)y + 4$	
f_{15}	$(1/4)x^4 + 5x^3y + (5/3)x^2y^2 + (1/10)xy^3 + (1/9)y^4 + x^3 + (2/3)x^2y + 9xy^2 + (1/8)y^3 + (7/10)x^2 + (1/5)xy +$ $(4/5)y^2 + (4/5)x + (5/8)y + 3/10$	
f_{16}	$(1/4)x^4 + 5x^3y + (5/3)x^2y^2 + (1/10)xy^3 + (1/9)y^4 + x^3 + (2/3)x^2y + 9xy^2 + (1/8)y^3 + (7/10)x^2 + (1/5)xy +$ $(4/5)y^2 + (4/5)x + (5/8)y - 97/10$	
f_{17}	$(1/4)x^4 + 5x^3y + (5/3)x^2y^2 + (1/10)xy^3 + (1/9)y^4 + x^3 + (2/3)x^2y + 9xy^2 + (1/8)y^3 + (7/10)x^2 + (1/5)xy +$ $(4/5)y^2 + (4/5)x + (5/8)y - 27/10$	
f_{18}	$-x^3 + y^2 + x$	
f_{19}	$-(1/5)x^3 + x^2y - (1/5)xy^2 + y^3 + (8/5)xy - 8y^2 - (12/5)x + 12y + 1/100$	
f_{20}	$(3/8)x^3 + 4x^2y + (10/7)xy^2 + (2/7)y^3 + x^2 + 10xy + (7/9)y^2 + (1/7)x + (4/5)y + 1687/300$	

Table 7: Polynomials defining curves

f_{21}	$(4/9)x^3+(10/7)x^2y+xy^2+(3/4)y^3+(7/2)x^2+8xy+(4/7)y^2+(4/3)x+(1/2)y+5/7$
f_{22}	$(1/4)x^5+2x^4y+(8/5)x^3y^2+(7/6)x^2y^3+(2/9)xy^4+(1/2)y^5+(3/5)x^4+8x^3y+5x^2y^2+(9/5)xy^3+2y^4+(7/10)x^3+7x^2y+9xy^2+2y^3+3x^2+4xy+(10/9)y^2+(10/3)x+(1/4)y+1/3$
f_{23}	$(8/3)x^3+(7/8)x^2y+(1/5)xy^2+(1/2)y^3+(1/2)x^2+8xy+6y^2+(5/4)x+5y+1/5$
f_{24}	$(1/5)x^3+x^2y+(7/4)xy^2+(4/5)y^3+(9/7)x^2+10xy+7y^2+2x+(7/10)y+5/8$
f_{25}	$(1/2)x^3+(3/2)x^2y+2xy^2+(2/9)y^3+x^2+9xy+(3/2)y^2+(6/7)x+(2/3)y+5/4$
f_{26}	$(3/8)x^3+4x^2y+(10/7)xy^2+(2/7)y^3+x^2+10xy+(7/9)y^2+(1/7)x+(4/5)y+1/3$
f_{27}	$(1/2)x^5+(9/4)x^4y+(8/5)x^3y^2+(5/7)x^2y^3+(4/3)xy^4+(1/8)y^5+(4/5)x^4+(2/5)x^3y+(8/5)x^2y^2+7xy^3+(2/3)y^4+(5/8)x^3+(3/7)x^2y+(9/7)xy^2+(3/5)y^3+x^2+(6/7)xy+(1/3)y^2+(1/2)x+(5/2)y-4/3$
f_{28}	$(1/2)x^5+(9/4)x^4y+(8/5)x^3y^2+(5/7)x^2y^3+(4/3)xy^4+(1/8)y^5+(4/5)x^4+(2/5)x^3y+(8/5)x^2y^2+7xy^3+(2/3)y^4+(5/8)x^3+(3/7)x^2y+(9/7)xy^2+(3/5)y^3+x^2+(6/7)xy+(1/3)y^2+(1/2)x+(5/2)y-8/15$
f_{29}	$(1/2)x^5+(9/4)x^4y+(8/5)x^3y^2+(5/7)x^2y^3+(4/3)xy^4+(1/8)y^5+(4/5)x^4+(2/5)x^3y+(8/5)x^2y^2+7xy^3+(2/3)y^4+(5/8)x^3+(3/7)x^2y+(9/7)xy^2+(3/5)y^3+x^2+(6/7)xy+(1/3)y^2+(1/2)x+(5/2)y+461/750$
f_{30}	$(7/9)x^4+(1/2)x^3y+(7/6)x^2y^2+(4/5)xy^3+(4/3)y^4+(2/7)x^3+(4/7)x^2y+(8/3)xy^2+(1/5)y^3+(7/10)x^2+(3/5)xy+(1/6)y^2+5x+(5/7)y+3/10$
f_{31}	$(3/10)x^4+(5/4)x^3y+(7/5)x^2y^2+(1/5)xy^3+y^4+(9/10)x^3+4x^2y+(2/9)xy^2+y^3+(3/4)x^2+(3/4)xy+y^2+(1/2)x+(9/2)y+9/8$
f_{32}	$4x^4+(1/2)x^3y+(1/9)x^2y^2+2xy^3+(9/7)y^4+9x^3+5x^2y+(5/3)xy^2+(4/3)y^3+(4/3)x^2+(5/2)xy+y^2+(1/3)x+(7/6)y+71/200$
f_{33}	$4x^4+(1/2)x^3y+(1/9)x^2y^2+2xy^3+(9/7)y^4+9x^3+5x^2y+(5/3)xy^2+(4/3)y^3+(4/3)x^2+(5/2)xy+y^2+(1/3)x+(7/6)y+3/8$
f_{34}	$(9/4)x^4+3x^3y+(1/7)x^2y^2+(2/7)xy^3+(1/3)y^4+(4/5)x^3+(1/5)x^2y+8xy^2+4y^3+2x^2+(10/9)xy+(5/3)y^2+(1/9)x+(1/5)y+2$
f_{35}	$(1/4)x^4+5x^3y+(5/3)x^2y^2+(1/10)xy^3+(1/9)y^4+x^3+(2/3)x^2y+9xy^2+(1/8)y^3+(7/10)x^2+(1/5)xy+(4/5)y^2+(4/5)x+(5/8)y+33/10$
f_{36}	$(1/5)x^4+(7/8)x^3y+(1/2)x^2y^2+(5/4)xy^3+y^4+(1/3)x^3+x^2y+8xy^2+y^3+(3/4)x^2+(5/7)xy+(5/9)y^2+(9/8)x+5y+4/3$
f_{37}	$(1/4)x^4+5x^3y+(5/3)x^2y^2+(1/10)xy^3+(1/9)y^4+x^3+(2/3)x^2y+9xy^2+(1/8)y^3+(7/10)x^2+(1/5)xy+(4/5)y^2+(4/5)x+(5/8)y+13/10$
f_{38}	$(1/7)x^3+(7/2)x^2y+(7/3)xy^2+(1/10)y^3+(6/7)x^2+9xy+(1/2)y^2+(7/5)x+y+1$
f_{39}	$(1/8)x^3+x^2y+2xy^2+(1/6)y^3+(6/7)x^2+9xy+(7/9)y^2+(1/9)x+(2/9)y+8/5$
f_{40}	$(1/10)x^3+(7/6)x^2y+(9/7)xy^2+(1/8)y^3+(9/4)x^2+10xy+2y^2+5x+(3/4)y+1/6$
f_{41}	$(1/4)x^4+(17/16)x^2y^2+(1/4)y^4-(5/4)x^2-(5/4)y^2+4382/7225$
f_{42}	$4x^4+(1/2)x^3y+(1/9)x^2y^2+2xy^3+(9/7)y^4+9x^3+5x^2y+(5/3)xy^2+(4/3)y^3+(4/3)x^2+(5/2)xy+y^2+(1/3)x+(7/6)y+7/8$
f_{43}	$4x^4+(1/2)x^3y+(1/9)x^2y^2+2xy^3+(9/7)y^4+9x^3+5x^2y+(5/3)xy^2+(4/3)y^3+(4/3)x^2+(5/2)xy+y^2+(1/3)x+(7/6)y+27/40$
f_{44}	$4x^4+(1/2)x^3y+(1/9)x^2y^2+2xy^3+(9/7)y^4+9x^3+5x^2y+(5/3)xy^2+(4/3)y^3+(4/3)x^2+(5/2)xy+y^2+(1/3)x+(7/6)y+19/40$
f_{45}	$(1/4)x^4+(17/16)x^2y^2+(1/4)y^4-(5/4)x^2-(5/4)y^2+40453/43350$

Code

Listing 1: minvol.m2

```

-- Calculate the Minkowski volume
-- of m*P1 + l*P2 + g*Delta for degree k
R = QQ[k, e_1..e_2, m_1..m_2][l_1..l_4]

K = (m_1 + m_2 + l_4)*k
L = (m_1*e_1 + m_2*e_2)
M = (l_4 + m_1)*k + m_2*(k - 1)

Vol = (K - L)^3 * (K + 3*L) - (K - M)^3 * (K + 3*M)

volToMvol = (substitutions) -> (
  vol := sub(Vol, substitutions);
  Mvol := (last coefficients (vol, Monomials => {l_1*l_2*l_3*l_4}))._0_0;
  Mvol = Mvol/4!; -- Compensate for the volume of the standard simplex
  assert (Mvol == k^4 - 5*k^2 + 4*k); -- Confirm we got the answer we expect
  return Mvol;
)

-- When k is even there is one copy of P1 (even monomials) and two of
-- P2 (odd monomials) and the other way around when k is odd.
({m_1 => l_1,      m_2 => l_2 + l_3, e_1 => 2, e_2 => 1},
 {m_1 => l_2 + l_3, m_2 => l_1,      e_1 => 1, e_2 => 2}) / volToMvol

```

Listing 2: lowDegreeBKK.m2

```

-- For m=2, 3 the polytopes do not have their general shape (and
-- aren't full dimensional either). However, the Minkowski sum /
-- mixed volume calculation still makes sense. So just do that for
-- these special cases.
needsPackage "PHCpack"

-- m = 2 case
g4 = (a^2 + b^2 + c^2 + d^2 + 1)
g1 = (c^2 + d^2)
g2 = (c + d)*(1 + a + b)

mv = mixedVolume {g1, g2, g2, g4}
assert (mv == 2^4 - 5*2^2 + 4*2)

-- m = 3 case
R = CC[a, b, c, d]
P4 = newtonPolytope

g4 = (a^3 + b^3 + c^3 + d^3 + 1)
g1 = ((c^2 + d^2)*(1 + a + b))
g2 = ((c + d)*(1 + a^2 + b^2) + (c^3 + d^3))

mv = mixedVolume {g1, g2, g2, g4}
assert (mv == 3^4 - 5*3^2 + 4*3)

```

Listing 3: numevidIdeal.m2

```
-- Numerical evidence for sharp BKK bound via degree counting.
S = QQ; load "preamble.m2"; D = 3; degreeSetup(D)

H = new MutableHashTable from {}

coeffs = unique toList apply(1..100, i -> randomCoefficients_D());
curves = coeffs / (c -> sub(abstractCurve_D, c));
fillIn_countSquares_H curves
tally values H
```

Listing 4: poging3.m2

```
S = QQ; load "preamble.m2"; D = 3; degreeSetup(D)

use ring abstractCurve_D
monomialTerms = terms sub(abstractCurve_D, validDegrees_D / (i -> C_i => 1))

curveThroughPoints = (N) -> (
  use ring abstractCurve_D;
  planePoints := toList(apply(1..N, i -> (random(S), random(S))));
  M := matrix (
    {monomialTerms}      | (planePoints /
      (p -> monomialTerms /
        (t -> sub(t, {X => p_0, Y => p_1})))));
  return determinant M;
);

H = new MutableHashTable from {};

curves = toList select(apply(1..20, i -> curveThroughPoints(9)), c -> 0 != c)
fillIn_(realSolutions_D @@ curveToCoeff_D)_H curves

pairs H / last / length
tally oo
```

Listing 5: preamble.m2

```
load "realroots.m2"
needsPackage "PHCpack"

W = S[a, b, c, d, MonomialSize => 8];
excess = ideal(c, d);
PHCring = CC[a, b, c, d];

sparseCoeffs = (coeff, localD) -> (
  H := new HashTable from coeff;
  -- Poor mans dict.update(H)
  return for deg in (validDegrees_localD / (d -> C_d)) list
    (if H#deg then (deg => H#deg) else (deg => 0));
);
```

```

zerofy = (squares) -> (
  squares / (square -> for x in square list
    if abs(x) < 1.0e-15 then 0.0 else x))
);

filterReal = (solutions) -> (
  return select(solutions / coordinates,
    j -> all(j, i -> 1.0e-90 > abs imaginaryPart i)) / (s -> s / realPart);
);

forMaple = (D, coeff, solss) -> (
  bounds := {"-10..10", "-10..10"};
  if length solss > 0 then (
    sols := solss / toList;
    Xen := flatten(sols /
      (s -> {s_0 + s_2, s_0 - s_2, s_0 + s_3, s_0 - s_3} ));
    Yen := flatten(sols /
      (s -> {s_1 + s_2, s_1 - s_2, s_1 + s_3, s_1 - s_3} ));
    bounds = (Xen, Yen) / (1 ->
      toString floor(-2 + min 1) | ".." | toString ceiling(2 + max 1));
  ) else (
    sols = [];
  );
  return "plotSquaresOnCurve" | toString ("(X, Y) -> " |
    toString sub(abstractCurve_D, coeff),
    " [X=" | bounds_0 | ", Y=" | bounds_1 | ", gridrefine=4] ",
    replace("\\}|\\|", "|", replace("\\{|\\|(", "[", toString sols))) | ";";
);

forMapleSimple = (curve, squares) -> (
  return "plotSquaresOnCurve((X, Y) -> " | toString curve | ", opts, " |
    replace("\\}|\\|", "|", replace("\\{|\\|(", "[", toString squares)) |")\n";
);

forMapleSequence = (curves, solutions) -> (
  assert(length curves == length solutions);
  contentS := toString(toList(
    apply(0..length(curves) - 1,
      i -> forMapleSimple(curves_i, solutions_i)))));
  return "opts := []; display(" | contentS | ", insequence=true);";
);

forMapleArray = (curves, solutions) -> (
  assert(length curves == length solutions);
  contentS := toString(toList(
    apply(0..length(curves) - 1,
      i -> forMapleSimple(curves_i, solutions_i)))));
  return "opts := []; display(Array([[" | contentS | "]], transpose));";
);

fillIn = (work, H, curves) -> (
  for curve in curves do (

```

```

    if not H #? curve then (
      result := work curve;
      H # curve = result;
    ) else (
      print ("Curve " | toString curve | " already present");
    );
  );
);

countSquares = (curve) -> (
  I := time saturate(makeIdeal_D curveToCoeff_D curve, excess);
  return (dim I, degree I);
);

degreeSetup = (D) -> (
  validDegrees_D = select(toList(
    set toList(0..D))^**2 / toList, d -> sum(d) <= D);
  R_D = S[apply(validDegrees_D, d -> C_d),
    MonomialSize => 8][a, b, c, d, MonomialSize => 8];
  T_D = R_D[X, Y];

  curveToCoeff_D = (curve) -> (
    sparseCoeffs(terms curve /
      (j -> C_(first exponents j) => leadCoefficient j), D);
  );

  use T_D;
  abstractCurve_D = sum(validDegrees_D / (d -> C_d * X^(d_0) * Y^(d_1)));
  use R_D;
  corners_D = {{ X => a + c, Y => b + d },
    { X => a - c, Y => b - d },
    { X => a + d, Y => b - c },
    { X => a - d, Y => b + c }} / (corner -> sub(abstractCurve_D, corner));
  IJ_D = ideal(
    corners_D_0 + corners_D_1 - corners_D_2 - corners_D_3,
    corners_D_0 - corners_D_1,
    corners_D_2 - corners_D_3,
    corners_D_3
  );
  -- FIXME: doing the saturation here is perhaps the wrong point.
  -- On the other hand, if we can store this computation, it might speed
  -- things up.

  randomCoefficients_D = () -> (
    return apply(validDegrees_D, s -> C_s => random(S))
  );

  makeIdeal_D = (coeff) -> (
    use W;
    I := sub(sub(IJ_D, coeff), W);
    J := I;
    return J;
  );

```

```

realSolutions_D = (coeff) -> (
  IP := sub(makeIdeal_D(coeff), PHCring);
  use PHCring; -- this is done to avoid the "key not found"
  complexSols := solveSystem IP_*;
  sols := unique zeroify filterReal complexSols;
  squares := select(sols, s -> s_2 >= 0 and s_3 > 0);
  if (length sols != 4 * length squares) then
    (
      print("Mismatch in solutions and squares " |
        toString (length sols, length squares));
      sols = unique zeroify filterReal refineSolutions(IP_*, complexSols, 18);
      squares = sort select(sols, s -> s_2 >= 0 and s_3 > 0);
    );
  return squares
);
)

```

Listing 6: drawSquares.mw

```

with(plots):
with(plottools):
with(RAGMaple):
SquarePegs:=module()
option package;
export plotSquare, plotSquaresOnCurve, componentsPoints;
local colorList;

componentsPoints := (curve) -> (
  seq(point([rhs(P[1]), rhs(P[2])]),
    P in PointsPerComponents([ curve = 0 ], [X, Y]))
);

plotSquare := proc(param, kleur)
  local a, b, c, d, p1, p2, p3, p4, line1, line2, line3, line4, plotOpts;
  (a, b, c, d) := op(param);
  plotOpts := thickness=2, color=kleur;
  p1 := [a + c, b + d]:
  p2 := [a - d, b + c]:
  p3 := [a - c, b - d]:
  p4 := [a + d, b - c]:
  display(CURVES([p1, p2, p3, p4, p1]), plotOpts):
end proc:

colorList := [
  navy, orange, plum, cyan,
  blue, green, black, maroon,
  gold, brown, pink, coral, magenta,
  khaki
];

plotSquaresOnCurve := proc(curve, curveOpts, squares,
  showComponents::boolean := true,
  showLegend::boolean := true)

```



```

local curvePlot, squaresPlot, setopts, xsX, ysY, passOpts,
    plotList, componentPoints;
setopts := [seq(lhs(o), o in curveOpts)];
passOpts := curveOpts;
if evalb(showComponents) then
    componentPoints := [seq(
        [rhs(P[1]), rhs(P[2])],
        P in PointsPerComponents([curve(X, Y) = 0], [X, Y])
    )];
else
    componentPoints := [];
end if;
if evalb(not X in setopts) then
    xsX := ListTools[Flatten](
        [seq([s[1] + s[3], s[1] + s[4], s[1] - s[3], s[1] - s[4]],
            s in squares)]
    );
    passOpts := [op(passOpts), X=-1+floor(min(xsX, seq(
        P[1], P in componentPoints)))..1
        +ceil(max(xsX, seq(P[1], P in componentPoints))
    )];
end if;
if evalb(not Y in setopts) then
    ysY := ListTools[Flatten](
        [seq([s[2] + s[3], s[2] + s[4], s[2] - s[3], s[2] - s[4]], s in squares
    )]);
    passOpts := [op(passOpts), Y=-1+floor(min(ysY, seq(
        P[2], P in componentPoints)))..1
        +ceil(max(ysY, seq(P[2], P in componentPoints))
    )];
end if;
if evalb(not gridrefine in setopts) then
    passOpts := [op(passOpts), gridrefine=4];
end if;
if evalb(showLegend) then
    curvePlot := implicitplot(curve(X, Y) = 0, op(passOpts),
        color=red, caption=typeset(curve(x, y), " inscribing ",
        nops(squares), " squares."):
else
    curvePlot := implicitplot(curve(X, Y) = 0, op(passOpts), color=red):
end if;
squaresPlot := [seq(plotSquare(squares[1 + i],
    colorList[1 + (i mod nops(colorList))])), i=0..nops(squares) - 1)];
if evalb(showComponents) then
    plotList := [curvePlot, op(squaresPlot),
        seq(point(P), P in componentPoints)];
else
    plotList := [curvePlot, op(squaresPlot)];
end if;
display(plotList, scaling=constrained):
end proc:

end module:

```